Time-resolved systems analysis of virus infection fate regulation

Mireia Pedragosa Marín

TESI DOCTORAL UPF / 2018

DIRECTORS DE LA TESI

Dr. Andreas Meyerhans i Dr. Jordi Argilaguet

DEPARTAMENT DE CIÈNCIES EXPERIMENTALS I DE LA SALUT

Als que estimo, i a les “Surullotes”,

ACKNOWLEDGEMENTS

Sembla mentida però per fi ha arribat el moment d'entregar i defensar la tesi. No m'ho puc ni creure… Així que toca agraïr a tots i totes els/les que han fet que això hagi estat posible.

To start with, I want to thank my supervisor Dr. Andreas Meyerhans, not only for providing a lab and money for the experiments, but also for his help during the thesis. I know I am not always easy and that I have still lots of things to learn… but I enjoyed (and will continue enjoying) the process.

Jordi, coneixent-me saps que, de tota la tesi, el que més m'està costant és aquest apartat… així que seré breu com sempre. INFINITES GRÀCIES PER TOT. Necessito una tesi sencera per poder agraïr-te tot el que has fet (I segur que hauràs de seguir fent, ho sento). Gràcies pel suport moral, mental i físic. I per cert, no m'oblido de la paella…

To all my labmates from the past and from the present. Gracielita (gracias por enseñarme Paraguayo Y por hacer del lab una fiesta), Vale, Eva, Kat, Mie, Javier, and the people from Juana's lab. You make from everyday a different and happy day, really.

A l'Eva, l'Erika, l'Òscar i a l'Àlex per la seva ajuda en els projectes de flow, que no sempre surt tot com una vol i per les xerrades "no tècniques" que fan les hores de flow més curtes.

A la meva família Petita i cuquetona, però única i divertida. Gràcies per aguantar els meus nervis (no els heu patit durant la tesi però si durant la carrera…). I a la Willy, que allà on sigui segur que està amb mi.

A l'Enric, per la paciència de cada dia i per ensenyar-me que els pigüins no volen, informació molt important per la tesi. I per acabar, a les meves nenes gordes, que apart de fer les seves necessitats també em fan moltíssima companyia.

Mireia,

Barcelona, Febrer 2018

SUMMARY

The processes and mechanisms of virus infection fate decisions that are the result of a dynamic virus - immune system interaction with either an efficient effector response and virus elimination or an alleviated immune response and chronic infection are poorly understood. Here, we characterized the host response to acute and chronic lymphocytic choriomeningitis virus (LCMV) infections by gene coexpression network analysis of time-resolved splenic transcriptomes. We found first, an early attenuation of inflammatory monocyte/macrophage prior to the onset of T cell exhaustion and second, a critical role of the XCL1-XCR1 communication axis during the functional adaptation of the T cell response to the chronic infection state. These findings not only reveal an important feedback mechanism that couples T cell exhaustion with the maintenance of a lower level of effector T cell response but also suggest therapy options to better control virus levels during the chronic infection phase.

RESUM

Encara són poc coneguts els processos i mecanismes resultants de la interacció dinàmica entre el virus i l'hoste que determinen que una infecció es resolgui favorablement gràcies a una resposta efectora eficient o que esdevingui crònica degut a l'atenuació de la resposta immunitària. En aquesta tesi, hem caracteritzat la resposta de l'hoste en front a una infecció aguda o crònica amb el virus de la coriomeningitis limfocítica (LCMV) mitjançant l'anàlisi de xarxes de coexpressió de gens derivades de transcriptomes de melsa. Els resultats obtinguts mostren, primer, una atenuació de monòcits/macròfags inflamatoris durant els primers dies després de la infecció i abans de que hi hagi esgotament de les cèl·lules T i, segon, un rol important de l'eix XCL1-XCR1 durant l'adaptació funcional de la resposta de cèl·lules T a la fase crònica de la infecció. Aquests descobriments, no només posen al descobert un mecanisme important de retroalimentació que uneix les cèl·lules T esgotades amb el manteniment d'un cert nivell de resposta efectora, sinó que també suggererixen noves opcions terapèutiques per intentar controlar la expansió del virus durant la fase crònica de la infecció.

PROLOGUE

The outcomes of viral infections are the result of dynamic interplays between an expanding virus and the concomitantly induced host immune responses. They can be categorized as either acute or persistent depending on temporal virus-host relationships. While acute infections are usually resolved within a few weeks, persistent infections are not resolved and develop when innate and adaptive immune responses are not sufficient to eliminate invading viruses during the primary infection phase.

A hallmark of an overwhelming infection is the downregulation of immune effector mechanisms to avoid immunopathology. Indeed, the simultaneous presence of a widespread virus infection and strong cytotoxic effector cell responses can induce massive cell and tissue destruction, and may directly threaten the life of the infected host. This threat is sensed by not completely understood mechanisms and several suppressive immune components are activated that adapt the host response to the viral threat. Amongst these are T cell exhaustion by deletion and functional impairment, the generation of monocyte-derived suppressor cells and regulatory cell subsets. Despite the various suppressive mechanisms induced during a chronic virus infection, the effector T cell shut-down is only partial and some T cell functionality remains that restrains the expansion of a persisting virus. The processes however that mediate the transition towards a lower level response are not well understood.

Viral infection fate is the result of complex temporal interactions between virus and host factors. However, most studies aiming to elucidate the immune components involved in infection fate regulation often focus in individual immune populations, and therefore a systems understanding of the early host response in acute and chronic infections is missing. In this thesis, I have used the well-established LCMV infection mouse model system to analyze on a systems level infection-fate–specific gene signatures and adaptive processes of the host to an overwhelming virological threat. The presented results contribute to better understand the complex virus-host interactions in acute and chronic infections, and provide a mechanistic understanding of the adaptation towards an overwhelming virus infection with both immunosuppressive and immunostimulatory processes that leave options for therapeutic interventions.

TABLE OF CONTENTS

INTRODUCTION

1. Chronic viral infections

1.1. Chronic viral infections: a persistent threat to human health

Viral infections can be fundamentally categorized as acute or persistent according to their temporal relationships with their hosts (Virgin et al. 2009). Acute infections in humans are usually resolved within a few weeks. By contrast, persistent infections are not resolved and, instead, develop when innate and adaptive immune responses are not sufficient to eliminate the invading virus during the primary infection phase. A consequence of this later condition is the establishment of a dynamic equilibrium between virus expansion and virus-specific adaptive responses that may be maintained stably for years without major pathological consequences or disrupted in a way that rapidly leads to overt disease. Viruses of both categories continue to threaten human health. Notable examples are the regular recurrences of Influenza virus strains that cause acute infections with partly critical illness or death every year (Fukuyama & Kawaoka 2011; Oldstone 2013) and chronic infections with the Human Immunodeficiency Virus (HIV) or the Hepatitis B and C viruses (HBV, HCV) that cause a tremendous disease burden with more than 500 million people infected worldwide. These viruses can establish persistence in their hosts with different probabilities and pathogenic consequences. Whilst nearly all HIV infections lead to virus persistence, 50-80% of HCV and only about 5% of HBV infections in adults are persistent. The level of persistence of HBV-infected newborns is massively increased to about 95% indicating that the state of the immune system is an important component in determining infection fate (Feinberg & Ahmed 2012; Rehermann & Nascimbeni 2005).

1.2. Immunological features of chronic infections

A number of viral and host factors in the early infection phase are involved in the fate decision between an acute and a chronic infection. Important factors include virus strain and escape variants (Zinkernagel 2002), viral dose and route of infection (Moskophidis et al. 1995; Asabe et al. 2009) and effector cell and virus expansion capacities (Bocharov et al. 2004; Ehl et al. 1998; Li et al. 2009). In the case of chronic infections, a decision is taken by the host in which the immune system undergoes a functional adaptation to a new virus-host equilibrium. Both suppressive and effector mechanisms participate in this immune adaptation, avoiding immunopathology while maintaining virus replication at low level (Wilson & Brooks 2010). A relevant feature of this adaptation is T cell exhaustion, defined as the deletion and functional impairment of virus-specific T cells (see section 2) (Moskophidis et al. 1993; Barber et al. 2006). Concomitant with T cell exhaustion, other regulatory elements also participate in the downregulation of the antiviral effector responses during chronic infections. Relevant

factors are IL10, regulatory T cells and myeloid derived suppressor cells (MDSCs) (see section 3.1) (Schmitz et al. 2013; Norris et al. 2013; Brooks, Trifilo, et al. 2006). The appearance of large numbers of MDSCs during chronic inflammation appears to be a common feedback mechanism in both mice and humans. In fact, MDSCs have been also documented in patients with HIV, were the number of MDSCs correlated positively with viral titers and regulatory T cells and negatively with the number of $CD4^+$ T cells (Vollbrecht et al. 2012). Finally, type I interferon signalling plays also an important role in facilitating virus persistence in chronic viral infections promoting T cell exhaustion. Indeed, blockade of interferons α/β (IFNα/β) receptor restores immune function and decreases viral loads in both lymphocytic choriomeningitis virus (LCMV) and HIV mice infection models (Teijaro et al. 2013; Wilson et al. 2013; L. Cheng et al. 2017; Zhen et al. 2017).

Besides the functional adaptation undergone by the immune system, several immunological abnormalities might affect innate and adaptive immune cell subsets in a chronic infection. Plasmacytoid dendritic cell (pDCs) functionality is disrupted in LCMV, HIV, and HBV chronic infections, affecting their capacity to produce IFNα and therefore affecting the overall immune response (Bergthaler et al. 2010; Macal et al. 2012; Fitzgerald-Bocarsly & Jacobs 2010). Conventional DCs functionality and maturation is also impaired, resulting in a reduced capacity to stimulate T cells (Fitzgerald-Bocarsly & Jacobs 2010; Sevilla et al. 2004). Also B cell and antibody responses are altered in many persistent infections (Ng et al. 2013), exhibiting a delayed production of virus-specific neutralizing antibodies and elevated levels of nonspecific antibodies (hypergammaglobulinemia) (Hunziker et al. 2003; Hangartner et al. 2006). Finally, another factor promoting immunological abnormalities is the disruption of the lymphoid tissue architecture mediated by collagen deposition and/or the loss of lymphoid stromal cells. This alteration impairs immune responses by affecting T cell survival and lymphocyte trafficking in immune tissues (Schacker et al. 2006; Zeng et al. 2012; Boehm 2016).

2. Exhaustion

2.1. General features of exhaustion

Exhaustion is a state of dysfunction that occurs as a consequence of antigen persistence (Pauken & Wherry 2015; Wherry 2011). It is a common feature of several persistent infections and cancers, but mainly studied in $CD8^+$ T cells in chronic viral infections. Exhaustion is associated with an altered metabolism and a unique

transcriptional program when compared with functional effector T cells and memory T cells. However, no master transcription factor of the exhausted transcriptional program has been identified to date (Wherry et al. 2007; Utzschneider et al. 2013; Crawford et al. 2014).

During exhaustion, $CD8^+$ T cell dysfunction develops in a progressive manner. Some functions are lost in an early stage of exhaustion, for instance high proliferative capacity and IL2 production. Other functions are lost in a more advanced stage of exhaustion such as cytotoxicity and TNFα and IFNγ production (Virgin et al. 2009; Wherry & John Wherry 2011). During exhaustion, T cells also lose their ability to proliferate in response to IL7 and IL15, thus depending on TCR signals for their maintenance (Shin et al. 2007). This process ultimately ends with the apoptosis of the exhausted cell (Kahan et al. 2015).

During chronic infections, exhaustion has been described as a causative factor for the lack of pathogen control. However, exhausted T cells still contribute to the containment of chronic infections (Kahan et al. 2015). Therefore, exhaustion might be an adaptation to reduce the sensitivity of virus-specific T cells to antigen and promote their survival in an antigen-rich environment. In this way, the immune response could balance effector control of the virus and immunopathology, while at the same time maintaining the adaptability of T cell responses to subsequent viral bursts (Radziewicz et al. 2009; Barnaba & Schinzari 2013; Pauken & Wherry 2015).

2.2. Intrinsic and extrinsic regulatory pathways of exhaustion

Exhaustion is associated with a prolonged and high expression of inhibitory receptors (Figure I1). The number and type of inhibitory receptors determine the degree of dysfunction. The pattern of inhibitory receptors differs between $CD4^+$ and $CD8^+$ T cells, as well as the type of infection. Inhibitory receptors involved in exhaustion include PD1 (which plays a major role), Lag3, Tim3, CD244 (2B4), CD160, TIGIT, CTLA4, BTLA, KLRG1 and others. However, none of these receptors are exclusive markers for exhausted T cells because activated T cells can transiently express them (Okoye et al. 2017; Crawford & Wherry 2009; Nguyen & Ohashi 2014).

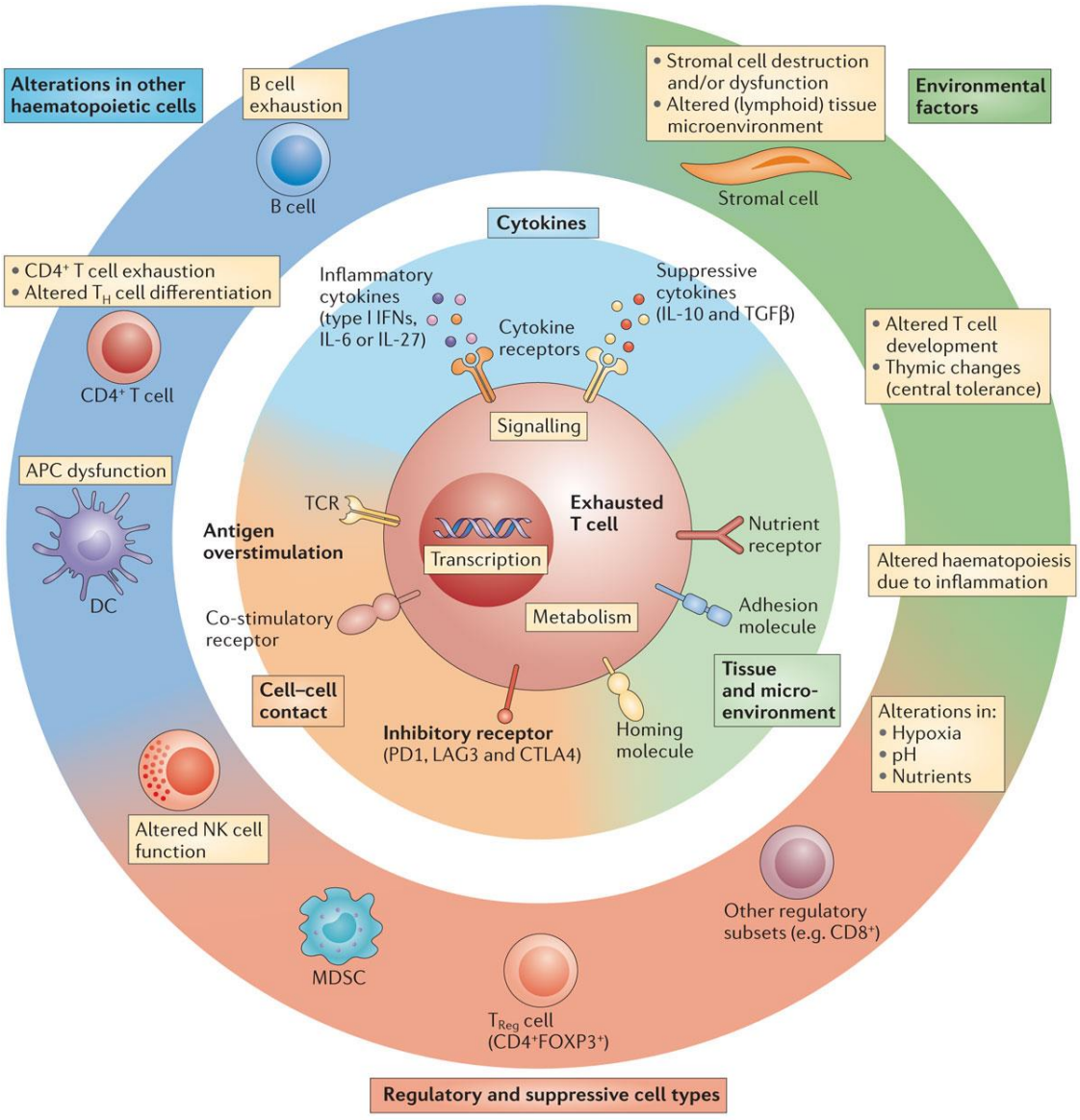

Figure I1. Overview of mechanisms of T cell exhaustion. Pathways implicated in T cell exhaustion can be classified into three general categories (centre and inner circle): cell-to-cell signals including prolonged T cell receptor (TCR) engagement (signal 1) and co-stimulatory and/or co-inhibitory signals (signal 2); soluble factors such as inflammatory cytokines (type I interferons (IFNs)) and suppressive cytokines including interleukin-10 (IL-10) and transforming growth factor-β (TGFβ); and tissue and microenvironmental influences driven by changes in the expression levels of chemokine receptors, adhesion molecules and nutrient receptors. Cell types such as antigen-presenting cells (APCs), CD4+ T cells, natural killer (NK) cells, B cells and regulatory cells (for example, myeloid-derived suppressor cells (MDSCs) and regulatory T (TReg) cells) have been implicated in CD8+ T cell exhaustion. From (Wherry and Kurachi 2015).

In addition to inhibitory receptors, multiple extrinsic factors influence T cell exhaustion, such as altered antigen presentation, immunosuppressive cytokines and several cell subsets (Wherry 2011; Jin et al. 2011; Kahan et al. 2015). Effector responses are influenced by deletion or alteration of dendritic cells, such as decrease

in MHC molecules and co-stimulatory ligands, and increase in co-inhibitory ligands (Jin et al. 2011). Likewise, effector responses are influenced by suppressive cytokines such as TGFβ and IL10 and inflammatory cytokines such as type I IFNs. For example, in the LCMV mouse model, the blockade of TGFβ (Jin et al. 2011; Tinoco et al. 2009) or IFN α/β during the first days of infection (Wilson et al. 2013; Teijaro et al. 2013) prevents from severe exhaustion, and the blockade of IL10 improves T cell functionality and promotes viral control (Brooks, McGavern, et al. 2006; Richter et al. 2013). In the case of HIV-infected individuals, as a result of PD1 triggering, monocytes produce IL10, which has been described as a major factor influencing effector impairment (Said et al. 2010).

In addition to all these factors, depletion of $CD4^+$ T cells is another important factor influencing exhaustion. $CD4^+$ T cells provide help to $CD8^+$ T cells and are major producers of IL21, which influences $CD8^+$ T cell and B cell differentiation and restricts regulatory T cell expansion (Matloubian et al. 1994; Zajac et al. 1998; Lichterfeld et al. 2004; Yi et al. 2009; Schmitz et al. 2013). On the contrary, NK cells and immunoregulatory cells such as MDSCs and regulatory T cells have a detrimental impact on virus-specific $CD8^+$ T cells further contributing to exhaustion (Dittmer et al. 2004; Dietze et al. 2011; Waggoner et al. 2011; Norris et al. 2013; Penaloza-MacMaster et al. 2014).

2.3. Maintenance of an effector response during chronic infection

Despite the various suppressive mechanisms induced during a chronic virus infection, the effector T cell shut-down is only partial and some T cell functionality remains to restrain the expansion of a persisting virus. In this sense, it has been shown that polyfunctional T cell responses in chronic HIV, HBV and HCV infections are linked to low viremia (Thimme et al. 2002; Bertoletti & Ferrari 2012; Hiroishi et al. 1997). Moreover, depletion of $CD8^+$ T cells in rhesus macaques infected with the simian immunodeficiency virus (SIV) results in an increase of virus loads (Schmitz et al. 1999; Jin et al. 1999). Finally, despite the presence of exhausted T cells, ongoing selection of virus mutants within epitope regions have been observed (Allen et al. 2005; Draenert et al. 2004). Recent studies characterizing $CD8^+$ T cell subsets that are present during chronic viral infection have identified a virus-specific population expressing the C-X-C chemokine receptor type 5 (CXCR5) that retain cytotoxic antiviral activities during chronic LCMV infection (Im et al. 2016; He et al. 2016; Leong et al. 2016) (Figure I2). Expression of the inhibitory receptors Tim3 and PD1 is slightly lower in $CXCR5^+$ $CD8^+$ T cells than in their $CXCR5^-$ counterparts, suggesting that these cells are less susceptible to exhaustion. In fact, $CXCR5^+$ $CD8^+$ T cells provide the proliferative burst after anti-PD1

therapy (Im et al. 2016). Importantly, HIV-infected patients also have a virus-specific $CXCR5^+$ $CD8^+$ T-cell subset, and its number inversely correlates with viral load (He et al. 2016). Thus, these studies define an unique subset of exhausted $CD8^+$ T cells that has a pivotal role in the control of viral replication during the chronic viral infection stage.

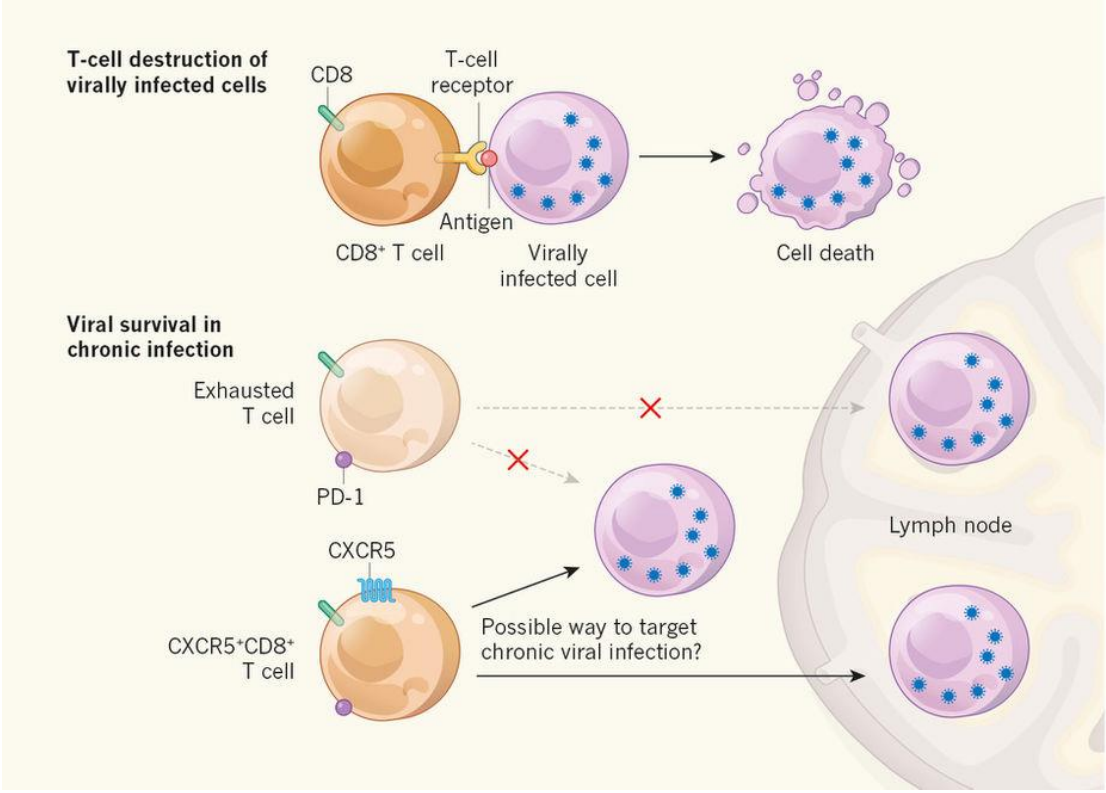

Figure I2. T cells that escape exhaustion. When a CD8+ T cell is exposed to a specific viral antigen that it recognizes through the T-cell receptor, the T cell becomes activated and can kill the virally infected cell presenting the antigen. In chronic infection, infected cells can escape T cell-mediated destruction if T cells enter an 'exhausted' state in which proteins such as PD1 inhibit T cell activation. Some studies have identified a population of activated CD8+ T cells that express the receptor protein CXCR5 and target chronic viral infection. These CXCR5+CD8+ T cells are not fully exhausted. From (Ma and Tangye 2016)

3. Immunotherapy to treat chronic viral infections

3.1. Reversing exhaustion

The exhausted phenotype of lymphocytes can be partially reversed. This was first shown in the LCMV model, in which the blockade of the PDD1/PDL1 pathway showed a restoration of impaired effector T cells and a reduction of viral loads (Barber et al. 2006). This observation was quickly extended (1) to HIV and HCV infections *in vitro* (Barber et al. 2006; Day et al. 2006; Trautmann et al. 2006; Urbani et al. 2006) (2) to

distinct infection models such as SIV in macaques, HCV in chimpanzees and HIV, HBV or *Plasmodium yoelii* in mice (Velu et al. 2008; Dyavar Shetty et al. 2012; Seung et al. 2013) and (3) to clinical trials in the case of HCV infection and several cancers (Yao et al. 2013; Nguyen & Ohashi 2014). Collectively, these results indicate that the PD1/PDL1 pathway plays a major role in exhaustion and represents a promising therapeutic target for chronic viral infections.

The restoration of exhausted T cells by the blockade of the PD1/PDL1 pathway is heterogenous. In the LCMV model, it has been reported that exhausted CD8 T cells with intermediate levels of PD1 expression can be reinvigorated, whereas $CD8^+$ T cells with high levels of PD1 cannot (Blackburn et al. 2008). This heterogeneity can be partly explained by the expression of multiple co-inhibitory receptors. Several studies showed that the simultaneous blockade of multiple co-inhibitory receptors increases considerably the restoration of impaired effector responses. Some of these combinations are PD1 and Lag3, PD1 and CTLA4, PD1 and Tim3, or PD1 and 2B4 (Blackburn et al. 2009; Nakamoto et al. 2009; Latchman et al. 2001; Jin et al. 2010).

3.2. Therapeutic vaccination

Therapeutic vaccination can offer an attractive method for boosting the immune response by reinvigorating exhausted $CD8^+$ T cells, and controlling the virus during persistent infections. Chronic infections are characterized by insufficient innate immune effector mechanisms that fail to eliminate the pathogen. The reasons for this failure are manifold and include immune shut-off mechanisms and viral escape from immune recognition. To overcome these difficulties, different strategies have been proposed. First, stimulation of molecules that positively regulate T cell responses. In this sense, costimulatory pathways such as CD40/CD40L, CD28/B7 or B7-2 have been identified and the use of their agonists as an adjuvant for therapeutic vaccines could enhance the effector function of exhausted $CD8^+$ T cells in chronic infection (Barr et al. 2006). Second, as explained in the previous sections of this thesis, exhausted $CD8^+$ T cells express inhibitory receptors such as PD1, and are also surrounded by an immunosuppressive environment, such as high levels of IL10. The combination of therapeutic vaccination and blockade of PD1 enhance $CD8^+$ T cell immunity and resolves LCMV infection in mice (Ha et al. 2008). Third, use of antigenically conserved epitope regions within the immunogen (Seddiki and Lévy 2018). This issue has been extensively discussed and considered within the context of HIV immunotherapies and several clinical trials are ongoing (Guardo et al. 2017). Taken together, several negative and suppressive pathways attenuate T cell immunity and lead to T cell exhaustion, and their blockade may be necessary to enhance therapeutic vaccination success.

4. Lymphocytic choriomeningitis virus: a mouse model for chronic infections

4.1. The virus

LCMV is the prototype virus of the arenavirus group that causes a persistent infection in its natural host, the mouse, but it can also infect a wide range of other animals, including humans. Although there is no quantitative data on the relative threats of the different LCMV virus strains to humans, it can cause a variety of syndromes that go from a mild respiratory infection to encephalitis or meningitis. Death from LCMV infection is rare, and patients usually recover without any sequelae (Farmer & Janeway 1942). Since its discovery in the early 1930s, infection of mice with several LCMV strains has been a widely used tool in scientific laboratories for examining mechanisms of viral persistence and basic concepts of virus-induced immunity and immunopathology (Wilson and Brooks 2010).

LCMV is an enveloped RNA virus with a bi-segmented negative single-stranded RNA genome. Its life cycle is restricted to the cytoplasm of the infected cell. Each of the RNA genome segments, designated as large (L, 7.3kb) and small (S, 3.5kb), uses an ambisense coding strategy to produce two viral gene products, in opposite orientation, and separated by a non-coding intergenic region (IRG) that folds in a stable hairpin structure (de la Torre 2009). The S RNA encodes the nucleoprotein (NP), the most abundant protein, and the viral glycoprotein precursor (GPC). The NP is the main structural element and plays an essential role in viral RNA synthesis. NP has been also associated with a type I interferon counteracting activity (Martínez-Sobrido et al. 2009; Martínez-Sobrido et al. 2007). The GPC is post-translationally cleaved into GP1 and GP2, and GP1/2 together make the spike of the virion. The L RNA segment encodes for the viral RNA dependent RNA polymerase (RdRp, or also referred as the L polymerase), and a small RING finger protein Z that localizes in the plasma membrane. The Z protein is a structural component of the virion that interacts with host proteins, inhibits RNA synthesis by the RdRp, and is the main driver of LCMV budding (de la Torre 2009).

The main cellular receptor for LCMV and other arenaviruses is the alpha-dystroglycan (α-DG) protein, a highly conserved and ubiquitous cell surface molecule that links the extracellular matrix with the cytoskeleton (Cao 1998; Kunz et al. 2003). Within immune cell populations, α-DG is mainly expressed by dendritic cells (DCs) (Oldstone & Campbell 2011). Virus strains and variants that bind α-DG with high affinity are associated with virus replication in the white pulp of the spleen, with preferential replication in DCs. LCMV infection of mature DCs has as consequence the failure of DCs

to present viral antigens and therefore to arm and expand immune-specific T and B cell responses (Oldstone & Campbell 2011). After interaction of α-DG with the viral GP1 a, LCMV virions are endocytosed. The subsequent fusion between the viral and cell membranes is triggered by the acidic environment found in the late endosome and GP2 (Gallaher et al. 2001). Upon release of viral genomic RNA, protein synthesis and genomic RNA replication starts. Formation and budding of arenavirus infectious progeny requires assembly of the viral ribonucleoproteins (RNPs) and the cellular membranes enriched with viral GPs. Finally, there is the assembly and cell release of the infectious virions (Perez & de la Torre 2003; Kunz et al. 2002).

4.2. LCMV contribution on viral immunology

The concept of persistent viral infection evolved from an observation Traub made in 1936. Mice infected with LCMV in the utero or shortly after birth neither died or eliminated the virus (Traub 1936a; Traub 1936b). In that time, three different LCMV isolates were originated: the Armstrong strain isolated from monkeys, the Traub strain isolated from a laboratory colony of persistently infected mice, and the WE strain, isolated from a human after exposure to persistently infected mice. Many different variants of these strains exist, but the most used are Clone 13, which derives from the Armstrong strain, and Docile, a derivative of the WE strain. LCMV infection fate varies dramatically depending on the virus strain, age and genetic background of mice, route of infection, as well as the dose used for infection (Spiropoulou et al. 2002; Zinkernagel 2002). In this sense, infection with low doses of LCMV Docile results in a rapid expansion of virus effector specific $CD8^+$ and $CD4^+$ T cells that clear the infection within 8-10 days postinfection (dpi). In contrast, infection with high doses of LCMV Docile results in clonal exhaustion of T cells and viral persistence (Cornberg et al. 2013a).

Since Traub's discovery in the 1930s, LCMV has been used as the preferred exploratory system and allowed numerous key findings about the innate and adaptive immune responses during acute and persistent viral infections. Some of these findings are the MHC-restricted action of the cytotoxic T cells (Buchmeier et al. 1980; Byrne et al. 1984), the understanding of T cell mediated cell lysis and particularly perforin-based cytotoxicity (Masson & Tschopp 1985), the emergence of the concept of adaptive immune memory which T cells "remember" their cognate antigen after initial antigen encounter (Murali-Krishna et al. 1998), and the implication of NK cells as master regulators of the $CD4^+$ T cell response which subsequently control $CD8^+$ T cell responses during viral infections (Waggoner et al. 2011). Besides the findings derived from basic viral immunology, multiple discoveries in the LCMV system have elucidated the mechanisms by which virus-specific T cells lose function allowing viral persistence, as well as the role of host immunoregulatory proteins such as PD1 in directly inhibiting

antiviral immune functionality and maintaining the immunosuppressive state (Barber et al. 2006; Okoye et al. 2017). The concept of immunopathology, that is the damage of tissues and organs due to the antiviral immune response rather than the virus itself, was also established in LCMV. Mediators of immunopathology include CTL, macrophages and neutrophils (Cole et al. 1972; Kim et al. 2009; Riviere et al. 1977).

4.3. Similarities between LCMV and HIV immunology

Although LCMV and HIV are two inherently different viruses, they elicit comparable antiviral responses. Both viruses initially trigger effector T cell responses as well as immunoregulatory strategies, but are unable to clear infection likely due to multiple factors including the selective loss of high affinity responders and continued propagation of functionally exhausted T cells (Lichterfeld et al. 2007; McMichael et al. 2010). For this reason, some of the immune features described in LCMV were then extended to the understanding of persistent HIV infection in humans (Klenerman & Hill 2005). Some examples are: (i) exhausted $CD8^+$ T cell responses in persistent LCMV infection mirror the ones found in HIV infection, including the increase of PD1 expression on virus-specific $CD8^+$ T cells (Barber et al. 2006). Moreover, PDL1 blockade resulted in an increase of CD8 T cells functionality in both viral infections (Day et al. 2006; Petrovas et al. 2006; Blackburn et al. 2008); (ii) increased IL10 production that causes T cell anergy and increased viral loads. Blockade of this cytokine enhances virus-specific T cell responses in both persistent LCMV infection and in HIV infected patients (Clerici et al. 1994; Landay et al. 1996); (iii) the need of $CD4^+$ T cell help for an optimal immune response to control virus replication (Matloubian et al. 1994; Battegay et al. 1994); (iv) IL2 expression is suppressed in both infections during the persistent phase of the infection (Pipkin et al. 2010), diminishing the expansion and generation of lasting memory $CD8^+$ T cells (Bachmann et al. 2007); and finally (v) IL21 produced by $CD4^+$ T cells is necessary for the maintenance of $CD8^+$ T cell effector responses during persistent LCMV infection (Fröhlich et al. 2009; Yi et al. 2009) as well as in HIV-infected patients (Yue et al. 2010). Thus, LCMV has been proven to be a valuable experimental tool to address meaningful mechanistic correlations between the mouse system and what one observes in human HIV infection.

5. Gene coexpression network analysis to study infection fate regulation

Viral infection fate is the result of complex temporal interactions between virus and host factors. However, due to technical reasons, most studies aiming to elucidate the immune components involved in infection fate regulation often focus in individual immune populations. Despite these studies are imprescindibles to our understanding of virus-host interactions, a systems understanding of the early host response in acute and chronic infections is missing and novel research aimed to shed light to the temporal relationships between the different events participating in infection fate is critical. As the technology towards high-throughput genomics is advancing and becomes more efficient and accessible, became possible the use of transcriptional profiling for system-level analysis. One of the methods increasingly used to explore the function of genes from a systemic point of view is the weighted gene correlation network analysis (WGCNA) (Figure I3).

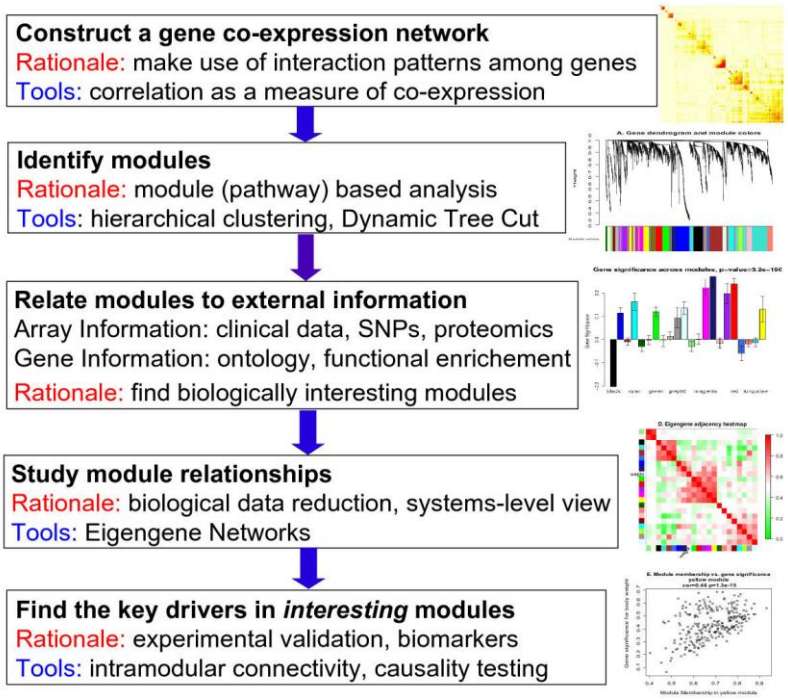

Figure I3. Overview of WGCNA methodology. This flowchart presents a brief overview of the main steps of Weighted Gene Co-expression Network Analysis. From (Langfelder and Horvath 2008).

In contrast with the traditional analyses of transcriptome data, WGCNA allows to understand the system instead of reporting a list of individual genes. This is accomplished by a biologically meaningful reduction of high dimensional data based on the identification of clusters (modules) of highly coexpressed genes sharing expression patterns. Analysis of these modules and their hub genes can provide insight into the underlying biological processes they represent (Langfelder & Horvath 2008). Three

major features of coexpression network analysis make this approach a valuable tool to analyze highly complex transcriptome data. First, the inclusion in the analysis of genes with low changes in their expression levels that might be highly connected to genes in a defined module. Second, the identification of trait-module relationships, permitting to characterize the molecular mechanisms underlying a phenotype of interest. And third, the analysis of the degree of preservation between modules from independent data sets, allowing the identification of highly conserved and highly-specific modules. WGCNA has been used at both cell and tissue levels, allowing to identify pathways associated with effector and exhausted CD8 + T cells (Doering et al. 2012), with different SIV infection phenotypes using whole blood transcriptome data (Yang 2016) and with hepatocellular carcinoma and breast cancer (Guo et al. 2017; Y. Cheng et al. 2017). Thus, bioinformatic analysis based on gene coexpression networks enables to extract the main temporal events that are involved in complex biological systems.

OBJECTIVES

The fate of a virus infection can be fundamentally categorized as acute or chronic according to its temporal relationship with the host organism. Despite the various suppressive mechanisms induced during a chronic virus infection, the effector T cell shut-down is only partial and some T cell functionality remains that restrains the expansion of a persisting virus. The processes however that mediate the transition towards a lower level response are not well understood. This thesis has 3 objectives:

1) To analyze on a systems level infection-fate-specific gene signatures.

2) To analyze the adaptive processes of the host to an overwhelming virological threat.

3) To generate hypotheses for therapeutic interventions to better control the invading virus.

MATERIALS AND METHODS

1. Media, buffer and solutions

Lysing solution

0.15M NH_4Cl (Merck), 10mM $KHCO_3$ (Sigma-Aldrich), 0.1mM Na_2EDTA (Sigma-Aldrich). pH 7,2-7,4.

FACS buffer

Phosphate buffered saline (PBS) (Gibco), 5% FCS, 0,5% Bovine serum albumin (Sigma-Aldrich), 0,07% sodium azide (Sigma-Aldrich).

FACS Fix buffer

Deionized water water, 1% paraformaldehyde (Sigma-Aldrich), 150mM NaCl (Sigma-Aldrich), pH7,4.

Complete RPMI

RPMI 1649 with L-glutamine (Sigma-Aldrich), 10% heat inactivated fetal calf serum (FCS) (Sigma-Aldrich), 1U/mL penicillin, 1µg/mL streptavidin, 0,05mM β-Mercaptoethanol, 1mM sodium pyruvate (Sigma-Aldrich).

Perm Wash buffer

Phosphate buffered saline (PBS) (Gibco), 1% fetal bovine serum (FCS), 0,1% NaN_3 (Sigma-Aldrich), 0,1% Saponine.

2. Animals and infections

Six- to twelve-week-old C57BL/6 (Charles River Laboratories) and XCR1-DTR-venus mice (Yamazaki et al. 2013a) were infected intraperitoneally (i.p.) with either $2x10^2$ or $1x10^6$ plaque forming units (PFU) of the strain Docile of LCMV ($LCMV_{DOC}$) to induce an acute or chronic infection, respectively. All animal work was conducted according to the guidelines from Generalitat de Catalunya and approved by the ethical committee for animal experimentation at Parc de Recerca Biomèdica de Barcelona (CEEA-PRBB, Spain).

3. Quantification of virus in tissue

Viral titers from spleens, lung and kidney of infected mice were determined by focus-forming assay (Battegay et al. 1991). A small piece of tissue was collected the day of necropsy and put directly at -80ºC until their use. For the assay, frozen tissues were smashed, resuspended in DMEM (Invitrogen), and serial dilutions were made. After,

200µL/well of the last three dilutions were plated in a 24 well plate (Sigma-Aldrich) containing 400,000 cells/well and were incubated for 4 hours at 37ºC. Once the cells formed a monolayer, a 1:1 mixture of 3% methocel (Sigma-Aldrich) and 2X DMEM (Invitrogen) was added into each well and incubated at 37ºC for 48 hours.

For the staining of plaque forming units, cells were fixed with 37% formaldehyde (Sigma-Aldrich), washed twice with PBS (Gibco), and incubated for 20 minutes with 1% TritonX solution (Sigma-Aldrich). For blocking non-specific bindings, cells were incubated 1 hour at RT with PBS containing 10% FCS. Cells were then incubated for 1 hour with VL4-rat anti-LCMV mouse antibody and 1 hour with anti-rat IgG HRP secondary antibody (Jackson ImmunoResearch). To visualize the plaques, DAB Peroxidase Substrare kit (Vector Laboratories) was used.

4. *In vivo* cell depletion

XCR1-DTR-venus mice have a fusion protein consisting of a diphtheria toxin receptor (DTR) and venus (a gene encoding a YFP derivative) into the *Xcr1* locus. For depletion of $XCR1^+$ dendritic cells (DCs), transgenic heterozygote and control mice received 25ng/g of body weight of Diphtheria toxin (DT, Sigma-Aldrich) at days 7, 10, and 13 postinfection (p.i.). Upon DT injection, $XCR1^+$ DCs were transiently and efficiently ablated. Physiological serum was used as a control vehicle.

5. Splenocytes isolation

Spleen samples were collected from mice and put directly in cold RPMI supplemented with 10% fetal bovine serum (FBS). If analysis of cytokines was needed, RPMI was also supplemented with Brefeldin A (10µg/ml), a protein transport inhibitor. After collection, spleens were homogenized into a single-cell suspension and filtered through a 40µm nylon cell strainer (Falcon) to remove clumps of cells. Splenocytes were then resuspended in ammonium chloride for 5 minutes at room temperature to lyse red blood cells, washed twice, and resuspended either in complete RPMI supplemented with 10% FBS for stimulation or cell sorting, or in FACS buffer for flow cytometry staining.

6. Cell staining and Flow cytometry

6.1 Splenocytes stimulation

For intracellular detection of IFN-ɣ, splenocytes were seeded at 1,5-2x10^6 cells/well in 96 wells round-bottom plates (Sigma-Aldrich) and incubated with either gp33 (1µg/ml) or gp61 (5µg/ml) peptides for two hours at 37ºC, respectively. In the case of CD107a and CD107b, the specific surface antibodies and the gp33 (1µg/ml) peptide were incubated together. After these two hours, 10 µL of brefeldin A (10µg/ml) was added and cells were further incubated for another three hours. After these incubations, cells were removed from the incubator and cell surface and intracellular staining was performed following the steps described in sections 6.2 and 6.3, respectively.

6.2 Cell staining

Splenocytes were seeded at 1,5-2x10^6 cells/well in 96 wells round-bottom plates (Sigma-Aldrich), washed twice with PBS and stained with a viability stain (Live/Dead fixable violet dye (Vivid) (Invitrogen) or Fixable viability stain 620 (BD biosciences) for 20 minutes at room temperature to exclude dead cells from the analysis. After, splenocytes were washed twice with FACS buffer and pelleted cells were then incubated for 20 minutes on ice in a total volume of 50µL with Fc block (BD Biosciences) to block non-antigen-specific binding of immunoglobulins to the Fc receptors. After blocking, cells were washed twice with FACS buffer and stained with 50µL of fluorochrome-labelled monoclonal antibodies against: CD4, CD8a, CD45R, CD11c, CD11b, MHCII, XCR1, NK1.1, Ly6G, Ly6C, CXCR5, PD1, Tim3, DbGP33-41$^+$ tetramer, and CD44. After surface antibody staining, cells were washed twice with FACS buffer and fixed with FACS fix. For intracellular staining, cells were permeabilized for 15 minutes with 100µL of Perm wash buffer. Once permeabilized, cells were washed twice with Perm wash buffer and pelleted cells were then incubated for 20 minutes on ice with 50µL of fluorochrome-labelled monoclonal antibodies against IFN-ɣ, IL-6 or XCL1. After, cells were washed with Perm wash and resuspended in FACS fix.

Stained cells were acquired in a flow cytometer within two hours after staining. Prior to acquisition cells were kept protected from light at 4ºC. Flow cytometry data were collected on a LSR Fortessa (BD biosciences) and analyzed with FlowJo software (Tree Star). Fluorescence minus one (FMOs) were done for PD1 and Tim3 to set the gates. Data were analyzed using FlowJo 10.1 software. Flow cytometry panels can be found in Table M1.

6.3 Sorting of monocytes/macrophages and DbGP33-41^{+}CD8^{+} T cells

For sorting of monocytes/macrophages and DbGP33-41^{+} CD8^{+} T cells, cells were seeded in polypropylene round bottom test tubes (Falcon) at 50x10^{6} cells/tube, rinsed with FACS buffer and incubated for 20 minutes on ice in a total volume of 100µL with Fc block (BD Biosciences) to block non-antigen-specific binding of immunoglobulins to the Fc receptors. Cells were then washed twice with FACS buffer and stained with 100µL of fluorochrome-labelled monoclonal antibodies against: CD45R, CD11c, CD11b, NK1.1, Ly6G, and Ly6C for monocyes/macrophages and with CD8, CD44, CXCR5, and DbGP33-41^{+} tetramer for CD8^{+} T cells. After surface antibody staining, cells were washed twice with FACS buffer and resuspend with RPMI supplemented with 10% FBS. Flow cytometry panels can be found in Table M1.

Stained Monocytes/macrophages and DbGP33-41^{+} CD8^{+} T cells were sorted in a FACSAria II SORP (BD Biosciences) right after staining. Sorted cells were collected in RLT buffer (Qiagen) and kept on ice during and after sorting. Sort purity was > 95% for all populations.

Table M1. Flow cytometry panels. (eBio: eBiosciences; BD: BD Biosciences; dil: dilution; Cat. nº: Catalog number)

IFNɣ in CD4^{+} and CD8^{+} T cells

Antigen	Fluorochrome	Company	Cat.nº	Clone	Volume
CD4	PE	BD	553653	H129.19	0,12µL
CD8	PECy5	BD	553034	536.7	0,12µL
INFɣ	FITC	BD	554411	XMG1.2	0,03µL

Monocytes/macrophages and neutrophils

Antigen	Fluorochrome	Company	Cat. nº	Clone	Volume*
Live/Dead	FVS620	BD	564996	-	Dil 1:1000
CD45R	PECF594	BD	562313	RA3-6B2	0,15µL
NK1.1	PECF594	BD	562864	PK136	0,3µL
CD11c	PerCP-Cy5.5	BD	560584	HL3	5µL
CD11b	APC	BD	553312	M1/70	0,625µL
Ly6G	PE	BD	551461	1A8	0,625µL
Ly6C	FITC	BD	561085	AL-21	0,625µL

*For sorting the volume of antibody was doubled and the quantity was tripled

IL-6 in Monocytes/macrophages

Antigen	Fluorochrome	Company	Cat. nº	Clone	Volume
Live/Dead	FVS620	BD	564996	-	Dil1:1000
CD45R	PECF594	BD	562313	RA3-6B2	0,15µL
NK1.1	PECF594	BD	562864	PK136	0,3µL
CD11c	PerCP-Cy5.5	BD	560584	HL3	5µL
CD11b	APC	BD	553312	M1/70	0,625µL
Ly6G	PE	BD	551461	1A8	0,625µL
IL6	FITC	eBio	11706181	MP520F3	1,25µL

Activated $CD8^+$ T cells

Antigen	Fluorochrome	Company	Cat. nº	Clone	Volume
CXCR5	APC	eBio	17718582	SPRCL5	0,625µL
CD8a	PerCP-Cy5.5	BD	551162	53-6.7	0,3µL
CD44	FITC	eBio	11044182	IM7	0,12µL
CD107a	PE	eBio	12107181	1D4B	1,25µL
CD107b	BV421	BD	564249	ABL-93	2,5µL

LCMV-specific $CD8^+$ T cells

Antigen	Fluorochrome	Company	Cat. nº	Clone	Volume*
Live/dead	FVS620	BD	564996	-	Dil 1:1000
CD8a	FITC	BD	553030	536.7	0,5µL
DbGP33	PE	MBL	MR03001	-	0,5µL
CD44	eFluor450	eBio	48044180	IM7	0,625µL
CXCR5	PE Cy7	eBio	25718580	SPRCL5	2,5µL

*For sorting the volume of antibody was doubled and the quantity was tripled

XCL1 production by NK cells and $CD8^+$ T cells

Antigen	Fluorochrome	Company	Cat. nº	Clone	Volume
Live/dead	Vivid	Invitrogen	L34955	-	Dil 1:5000
NK1.1	PECF594	BD	562864	PK136	0,3µL
CD3e	PE Cy7	BD	561100	1452C11	1,25µL
CD8a	FITC	BD	553030	53-6.7	0,5µL
CD4	PE	BD	553048	RM 4-5	0,01µL
XCL1	-	R&D	MAB486	80222	0,5µL
Anti-rat IgG2a	AF647	abcam	Ab172333	2A8F4	Dil. 1:2000

XCL1 production by LCMV-specific CD8$^+$ T cells

Antigen	Fluorochrome	Company	Cat. nº	Clone	Volume
Live/dead	FVS620	BD	564996	-	Dil 1:1000
CD8a	FITC	BD	553030	536.7	0,5µL
DbGP33	PE	MBL	MR03001	-	0,5µL
CD44	eFluor450	eBio	48044180	IM7	0,625µL
CXCR5	PE Cy7	eBio	25718580	SPRCL5	2,5µL
XCL1	-	R&D	MAB486	80222	0,5µL
Anti-rat IgG2a	AF647	abcam	Ab172333	2A8F4	Dil 1:2000

Exhausted CD8$^+$ T cells

Antigen	Fluorochrome	Company	Cat. nº	Clone	Volume
Live/dead	FVS620	BD	564996	-	Dil 1:1000
CD8a	PerCP Cy5.5	BD	551162	53-6.7	0,3µL
CXCR5	PE Cy7	eBio	25718580	SPRCL5	2,5µL
CD44	eFluor450	eBio	48044180	IM7	0,625µL
DbGP33	PE	MBL	MR03001	-	0,5µL
PD1	FITC	eBio	11998581	J43	1,25µL
Tim3	APC	Biolegend	134007	B8.2C12	2µL

XCR1$^+$ Dendritic cells

Antigen	Fluorochrome	Company	Cat. nº	Clone	Volume
Live/dead	Vivid	Invitrogen	L34955	-	Dil1:5000
CD45R	PECF594	BD	562313	RA36B2	0,15µL
CD11c	PerCP Cy5.5	BD	560584	HL3	5µL
CD8a	FITC	BD	553030	53-6.7	0,5µL
XCR1	BV510	Biolegend	148218	ZET	2,5µL

7. Immunohistochemistry

Spleen samples for immunohistochemistry were embedded in paraffin after an overnight fixation with 4% buffered formaldehyde. Three micrometer thick tissue sections were deparaffinized and rehydrated before staining with Mayer's Hematoxylin and Eosin. Extra sections were obtained and were incubated with DAKO EnVision+ System HRP labelled polymer with anti-Mouse IgG for immunohistochemical labelling and semiquantification of IgG-positive cells. The reaction was visualized using hydrogen peroxide and 3-3'-diaminobenzidine as a chromogen substrate. A set of

scores was defined from 0 (absence of immunolabeled cells in the studied sections) to 10 (100% IgG labelled cells in the studied sections). For semiquantification of fibrosis, spleen sections were stained with Masson's Trichrome staining, which stains collagen fibers in color blue. A set of values was defined from 0 to 10: a score of 0 represents normality (a certain amount of blue stained collagen is to be observed in the splenic capsule and trabeculae); a score of 10 would correspond to a spleen in which the parenchyma has totally been replaced by connective tissue.

8. RNA isolation and quantitative real-time PCR

Total RNA from spleens (15-20 mg) and sorted cells ($5x10^4$ cells per sample) was isolated, including DNAse (Quiagen) treatment, according to the manufacturer's instructions using Qiagen RNeasy Mini kit for spleen tissue and Qiagen RNeasy Micro kit for sorted cells (Qiagen), respectively. The quality and concentration of RNA were determined by an Agilent Bioanalyzer. Good quality RNA (50ng) was used to generate a cDNA template using SuperScript III Reverse Transcriptase (ThermoFisher). Quantitative real-time PCR was performed in a total volume of 15 µL that includes 50ng of cDNA, forward and reverse primers at a concentration of 0.2 µM, and 7.5 µL of SYBR select master mix (ThermoFisher). Each reaction was performed in triplicate in a 384 well plate (Sigma-Aldrich) in a Quantstudio 12K flex (ThermoFisher) using the following parameters: 2 min 50°C, 95°C 10 min, 40 cycles of 15 sec at 95°C and 60 sec at 60°C. Primers for all genes were designed using the program Primer Express 3.0 (Applied Biosystems). Primer selection parameters were as follows: primer size between 10 and 40 nucleotides; primer melting temperature from 52ºC to 60ºC; GC content between 40% and 60%; and product size between 150 and 250 nucleotides. Primers were ordered from Biomers. Sequences for the primers used can be found in Table M2.

Table M2. Primer sequence

Gene	Strand	Sequence
Gapdh	Forward	5'-CCA GTA TGA CTC CAC TCA CG-3'
	Reverse	5'-GAC TCC ACG ACA TAC TCA GC-3'
Xcl1	Forward	5'-TTT GTC ACC AAA CGA GGA CTA AA-3'
	Reverse	5'-CCA GTC AGG GTT ATC GCT GTG-3'
Il6	Forward	5'-TGG GAC TGA TGC TGG TGA CA-3'
	Reverse	5'-TTT CCA CGA TTT CCC AGA GAA-3'
Il1ß	Forward	5'-GGA GCT CCC TTT TCG TGA ATG-3'
	Reverse	5'-TCT TGG CCG AGG ACT AAG GA-3'

Nos2	Forward	5’-ACT CTT CAC CAC AAG GCC ACA T-3’
	Reverse	5’-GTT GAT GAA CTC AAT GGC ATG AG-3’
Itgb2	Forward	5’-AGC CAC CGA TGT GTG AGG AT-3’
	Reverse	5’-AAG GGA TAG TCT GCA GCG TCA T-3’
Ccr1	Forward	5’-CTC ATG CAG CAT AGG AGG CTT-3’
	Reverse	5’-ACA TGG CAT CAC CAA AAA TCC A-3’
C5ar1	Forward	5’-TAC CAT TAG TGC CGA CCG TTT-3’
	Reverse	5’- CCG GTA CAC GAA GGA TGG AAT-3’
Itgam	Forward	5’-GCA CCA AAA CTG CAA GGA GAA-3’
	Reverse	5’-CCG GAG CCA TCA ATC AAG AA-3’
Zap70	Forward	5’- TCG GCA CTA TGC CAA GAT CA -3’
	Reverse	5’-TCA CTG CGG CTG GAG AAC TT -3’
Cd3d	Forward	5’-GTG GAA GGA TGG TTT GCA AA-3’
	Reverse	5’- CAC ACA GTT CTG GCA CAT TCG -3’
Cd3e	Forward	5’- CCA GCG GGA CCT GTA TTC TG -3’
	Reverse	5’ - AAC AAG GAG TAG CAG GGT GC -3’
Fut8	Forward	5’- GTT ATT GGA GTC CAT GTC AG -3’
	Reverse	5’- TTG GAG TAC TTT GTC TTT GC -3’
Ighg2c	Forward	5’- TGA TTG TGC AGA CCC TCG TG -3’
	Reverse	5’- CTG TGG ACT GGA CCA GCA AT -3’
Cd247	Forward	5’- GCT GGA TCC CAA ACT CTG CT -3’
	Reverse	5’- GCT GTT TGC CTC CCA TCT CT -3’

9. Bioinformatic analysis

9.1 RNA-seq library preparation and sequencing

Sequencing libraries were obtained after removing ribosomal RNA by a Ribo-Zero kit (Illumina). cDNA was synthesized and tagged by addition of barcoded Truseq adapters. Libraries were quantified using the KAPA Library Quantification Kit (KapaBiosystems) prior to amplification with Illumina’s cBot. Four libraries were pooled and sequenced (single strand, 50nts) on an Illumina HiSeq2000 sequencer to obtain 50-60 million reads per sample.

9.2 RNA-seq bioinformatic analysis

Reads mapping against the Mus musculus reference genome (GRCm38) was done using the GEMtools RNA-seq pipeline (http://gemtools.github.io/docs/rna_pipeline.html), and were quantified with Flux Capacitor (http://sammeth.net/confluence/display/FLUX/Home) with the Mus musculus gencode annotation M2 version (https://www.gencodegenes.org/). Normalization was performed with the edgeR TMM method (Robinson & Oshlack 2010). Pairwise Pearson's correlation coefficients (PCC) were calculated for comparison among transcriptomes of spleens from uninfected (n=2, day 0), acute (n=2 per time point) or chronic (n=2 per time point) infected mice. Hierarchical clustering across all samples was based on pairwise Pearson's correlation coefficients among RNA-seq libraries. Differential expression analysis was performed with the 'robust' version of the edgeR R package (Zhou et al. 2014). Genes with a false discovery rate (FDR)<5% were considered significant. Differentially expressed genes in acute and chronic time series (n=13971) were used to construct a coexpression network with the WGCNA R package for each dataset (Langfelder & Horvath 2008). First, a signed weighted adjacency matrix was calculated with the 'blockwiseModules' function using these parameters: power=30, TOMtype="signed", minModuleSize=15, mergeCutHeight=0.25, reassignThreshold=0, networkType="signed", numericLabels=TRUE, pamRespectsDendro=FALSE, nThreads=7, maxBlockSize=17000. The power law of 30 was selected to meet the scale-free topology assumption with the pickSoftThreshold function. Then, genes were clustered into network modules using average linkage hierarchical clustering and the topological overlap measure (TOM) as proximity. Each of the identified modules was summarized by its module eigengene (the first principal component), which represents the weighted average expression profile of all module genes (Langfelder & Horvath 2008). To identify intramodular hub genes inside a given module, the intramodular connectivity was calculated for each gene (Kin) and ViSANT (http://visant.bu.edu/) was employed for network visualizations (TOM>0.3). Module preservation and module overlapping were calculated with functions 'modulePreservation' and 'userListEnrichment', respectively. Viral loads, CD4 and CD8 levels were correlated with the module eigengenes with Pearson correlation. Gene ontology (GO) enrichment analysis was performed with DAVID (http://david.ncifcrf.gov/) (Huang et al. 2009).

9.3 Module preservation analysis

Z-summary, implemented within WGCNA, with 100 random permutations of the data, is used as a connectivity-based preservation statistic able to determine whether the connectivity pattern between genes in a reference network is similar to that in a test network. A Z-summary score < 2 indicates no evidence of preservation, 2 < Z-summary < 10 implies weak preservation and Z-summary > 10 suggests strong preservation. Highly preserved modules were defined as those with a preservation Z-summary value above 10 and percentage of differentially connected genes below 20%. Group-specific modules were defined as those with a preservation Z-summary value below 2 and a percentage of differentially connected genes above 35%.

10. Statistical analysis

Two-tailed t test or one-way ANOVA analyses were performed using GraphPad Prism 6.0 (San Diego, CA, USA). pvalues (p) below 0.05 were considered significant and were indicated by asterisks: *$p \leq 0.05$; **$p \leq 0.01$; ***$p \leq 0.001$; ****$p \leq 0.0001$. Non-significant differences were indicated as “ns”.

RESULTS

1. Spleen gene coexpression networks in acute and chronic viral infections

The development of an acute or a chronic virus infection is the result of a coordinated response of the immune system towards the invading microbe. While several of the individual components that contribute to this fate decision have been described, a systemic global view is still lacking. Thus, we characterized transcriptome changes at the level of the spleen during the course of viral infections with different outcomes. C57BL/6 mice were infected with a low-dose ($2x10^2$ PFU; acute infection) or a high-dose ($2x10^6$ PFU; chronic infection) of LCMV strain Docile ($LCMV_{Doc}$). Virus titers, virus-specific $CD4^+$ and $CD8^+$ T cell responses, and spleen-derived total messenger RNAs (mRNAs) were determined longitudinally by titration, intracellular cytokine staining (ICS) and RNA-seq, respectively. Due to the different inoculum size, virus titers in spleen increased later in acute than in chronic infection, however similar levels were observed at d5 postinfection (p.i.) (Figure R1A). As previously described (Moskophidis et al. 1993), low-dose infection resulted in virus clearance while high-dose infection led to virus persistence shown as high viral titers in spleen at d31 p.i.. The IFNγ-producing T cells expanded at d6-d7 and their percentages remained high at d31 when virus was undetectable after low-dose infection (Figures R1B and S1A). In high-dose infected mice, IFNγ-producing $CD8^+$ T cells also increased at d6-d7 p.i. however their number dropped at d7-d9, which is indicative of $CD8^+$ T cell exhaustion.

To characterize changes of transcriptional profiles from spleens during acute or chronic infection, we isolated total mRNAs from naive mice (d0) and from mice at d3, d5, d6, d7, d9 and d31 after low-dose or high-dose of $LCMV_{Doc}$ infection, and determined time-resolved transcriptomes by RNA-seq. Hierarchical clustering across all samples revealed four main groups corresponding to different infection phases (Figure R1C). The first group, naive mice and mice in memory phase, is represented by samples from acute infected mice at days 3 and 31, and uninfected mice (d0), indicating that spleen transcriptome profiles return to that of naive mice once the infection is resolved. Early effector responses (group 2) and late effector responses (group 3) are represented by samples from d5-d6 of acute plus d3 of chronic infection and d7-d9 of acute plus d5-d7 of chronic infection, respectively. This indicates that at a tissue level, central host responses are similar in acute and chronic infections albeit, due to the different inoculum size, they appear at different time points. Finally, d9 and d31 samples from chronic infection, that is once $CD8^+$ T cell exhaustion is established, cluster in a separate group 4 representing a specific chronic infection phase. Thus, distinct virus infection phases exhibit separated transcriptome signatures in the lymphoid tissue.

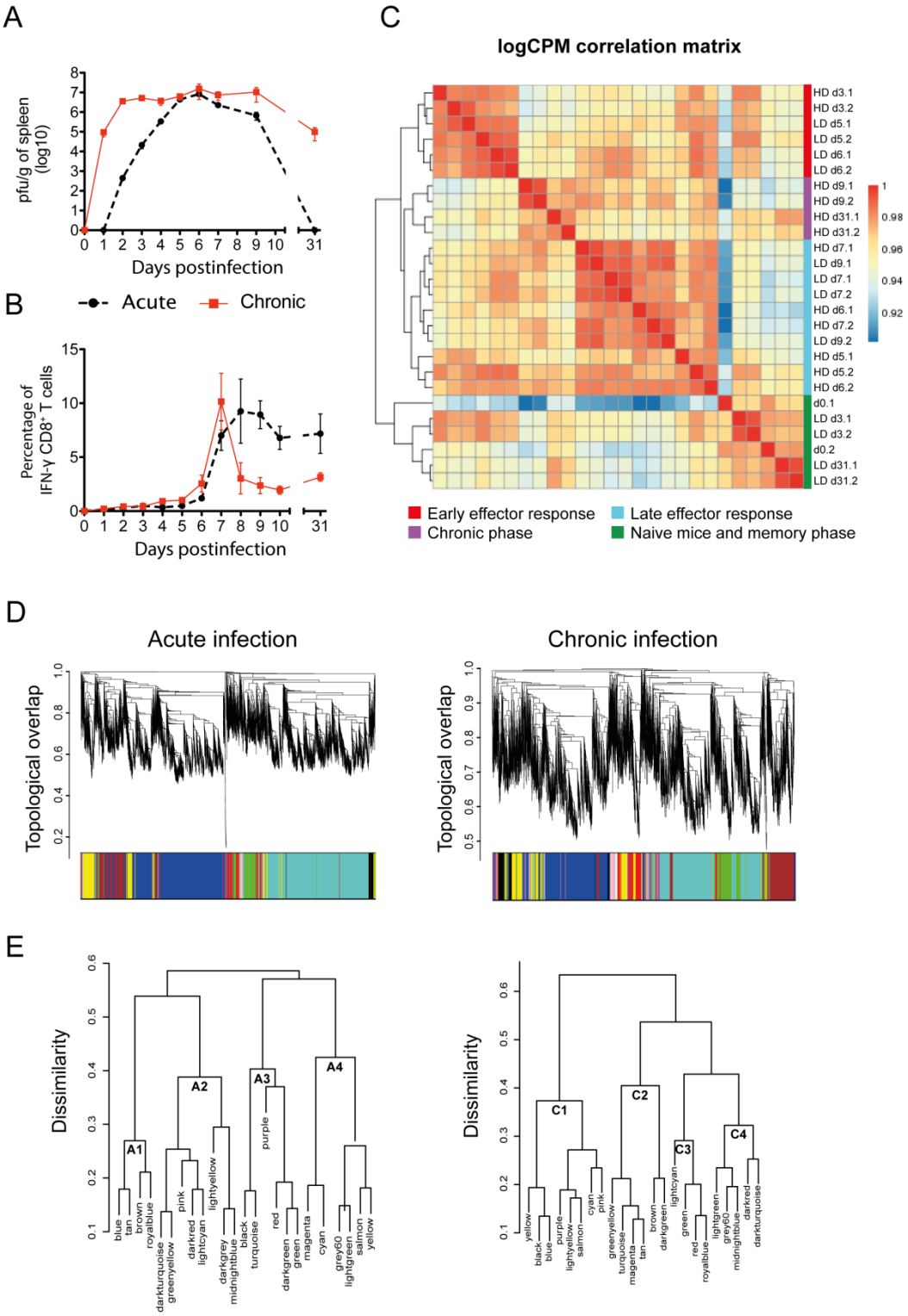

Figure R1. Kinetics of virus expansion, CD8$^+$ T cell response, and transcriptome analysis in LCMV infections. (A and B) Virus titers (A) and percentages of GP33-specific IFNγ-producing CD8$^+$ T cells (B) in spleen. The mean ± SEM is shown. (C) Correlation matrix heatmap of gene expression across LD and HD samples. The color scale indicates the degree of correlation. (D) Hierarchical clustering dendrogram for all differentially expressed genes (lines) obtained by WGCNA. The branches correspond to modules of highly coexpressed groups of genes. Colors below the dendrogram indicate the module that each gene was assigned to. (E) Hierarchical clustering dendrogram of dissimilarity based on module eigengenes.

Taking non-infected mice as a reference point, the analysis of differentially expressed genes after acute and chronic infection showed a similar number of up- and down-regulated genes from d5 to d9 (Figure S1B). Appreciable differences between both types of infection were found only at early (d3) and late (d31) time points when acute infected mice showed fewer differentially expressed genes. This reflects the different host response kinetics between the two types of infection at early time points and the continuous deviation of the chronic infection state from the basal level of transcription of naive mice. Gene Ontology (GO) analysis showed identical enriched terms in acute and chronic infections representing general biological processes such as “cell cycle”, “immune response”, and “programmed cell death”.

To explore the dynamics of the spleen transcriptomes during both infection courses we applied weighted gene correlation network analysis (WGCNA) and constructed two signed coexpression networks (Zhang & Horvath 2005). Topological overlap was used to measure the connection strength between genes based on shared network neighbours, identifying genes with similar patterns of connections and subsequently defining modules of highly coexpressed genes (Figure R1D). Finally, the eigengene was extracted for each module to represent the gene expression profile. 23 modules were identified from acute and chronic infections (Figure S1C). They were color-coded for identification purposes. Of note is that the same colour in modules from acute and chronic networks does not imply any similarity between them. The number of genes per module ranged from 15 to 4952 (Figure S3A).

To obtain a global view on the similarity of the module expression patterns we generated a hierarchical clustering dendrogram based on module’s eigengenes and defined 4 clusters for each infection outcome (A1 to A4, acute infection; C1 to C4, chronic infection) (Figures R1E and S1C). Clusters A1, A4 and C2 include modules with upregulated expression profiles at d3-d7 p.i. reflecting the complexity of the host effector response while the modules from clusters A3 and C1 show an early downregulation of expression. Clusters A2 and C4 contain modules with “two-peak” expression profiles having the first peak at an early time point postinfection when the host response is triggered and a second peak at d9 when the infection outcome is already determined. Finally, the expression pattern of the modules from cluster C3 was characteristic of chronic infection showing an initial downregulation but subsequent gradual upregulation until d31.

2. Cellular and humoral adaptive responses are disassociated in chronic infection

The determined time-resolved global spleen transcriptomes revealed the extraordinary complexity of the host response against acute and chronic infections. While we could decompose this complexity to modules of highly coexpressed genes using WGCNA, their link to biological processes had to be established and proven. $CD8^+$ T cells play a major role in the control of an LCMV infection as well as in exhaustion during chronic infections (Oldstone 2006). We therefore tested whether the behavior of virus-specific T cells was mirrored by a gene expression pattern of similar kinetics. For this we correlated the module eigengenes with the kinetics of IFNγ-producing GP33-specific $CD8^+$ T cells (Figure S2A). The acute-brown module significantly correlated with the virus-specific $CD8^+$ and $CD4^+$ T cell responses of acute infection (Figure R2A). To visualize this correlation at the level of the individual genes, we compared the intramodular connectivity (K_{IM}) of each gene of this module with its correlation to the T cell response. A correlation was observed indicating a link between the hub genes (high K_{IM} values) to the T cell response (Figure R2B). In contrast, no significant correlation between chronic-module eigengenes and the virus-specific $CD8^+$ T cell response of chronic infection was observed (Figure S2A).

Hub genes from coexpression modules are defined by a high K_{IM} value, or alternatively by a high topological overlap, and are predicted to be central for the biological processes they represent (Jeong et al. 2001; Doering et al. 2012). Thus, we visualized the hub genes of the acute-brown module as a network based on their topological overlap values (Figure R2C). Two clusters were observed that are enriched in the GO terms TCR signalling pathway, vesicle-mediated transport, inflammatory response, and B cell response. Cluster 1 contains key genes in T cell activation and Cluster 2 contains genes from the B cell response. To analyse how these hub genes in acute infection behave during chronic infection, we compared their intramodular connectivities in both infection outcomes (Figure S2B). Genes from cluster 1 related to T cell activation were found in two different chronic modules, chronic-tan and chronic-greenyellow (Figure S2B). However, only genes in chronic-tan retained a $K_{IM}>0.6$ and therefore represented control points of T cell activation in chronic infection. These genes were upregulated at day 6 and returned to basal levels at day 31 thus having a similar kinetics as in acute infection (Figure R2D). In contrast, genes in the chronic-greenyellow module showed an upregulation at day 6 with a subsequent downregulation at day 9 thus coinciding with T cell exhaustion. To validate these observations and to link the day 9 downregulation of the chronic-greenyellow genes to T cell exhaustion, we performed qPCR of selected genes from spleens of mice at day 9

after acute or chronic infection (Figure S2C and S2D). The qPCR results positively correlated with the RNA-seq data. CD3d and ZAP70 from the chronic-greenyellow module that play a critical role in T cell receptor signaling and that were chosen as examples, were significantly downregulated in chronic infection thus supporting a role during T cell exhaustion.

The B cell response-related genes of cluster 2 were mainly found in the chronic-green module and retained a high intramodular connectivity value (Figure S2B, right panel). Thus, the B cell response during both infection types is controlled by a highly coregulated gene expression. The expression kinetics of these genes during acute and chronic infections were identical, being upregulated from d7 to d9 and remaining elevated at d31. However, their expression levels were notably higher in chronic infection (Figure R2E and Figure S2D) suggesting a causal link to the previously described hypergammaglobulinemia of chronic infections (Hunziker et al., 2003). To validate this, spleens from acute and chronic LCMV infections were stained for total IgG and analyzed by immunohistochemistry. IgG production was evident at d9 in both types of infection but was significantly higher in chronic infection. An elevated level of IgG remained visible even at day 48 postinfection when the B cell response of acute infection was comparable to that of naive mice (Figure R2F and R2G). Taken together, coexpression network analysis from spleen-derived transcriptomes permits the identification of biologically relevant molecular pathways that are characteristic for acute or chronic infections. They should therefore enable the identification of novel key features implicated in infection outcomes and its regulation

Figure R2. Genes related to T and B cell responses from the acute-brown module are disassociated in chronic infection. (A) Acute-brown module eigengene and kinetics of GP33-specific $CD8^+$ and GP61-specific $CD4^+$ T cells. (B) Intramodular connectivity versus GP33-specific $CD8^+$ T cell kinetics correlation significance for acute-brown module genes. (C) Visualization of the acute-brown module genes. Large nodes represent hub genes with high connection densities (TOM>0.5). (D and E) Expression kinetics of acute-brown module genes related to T cell activation (D) and hub genes related to the B cell response (E) in acute and chronic infections. (F) Representative images of IgG immunohistochemical staining of spleens. Magnification bar: 100µm. (G) Semiquantification of IgG-positive cells in spleens (score 0-10). Data shown are mean ± SEM of 4 mice per group and time point. *** $p \leq 0.001$ (unpaired two-tailed t test).

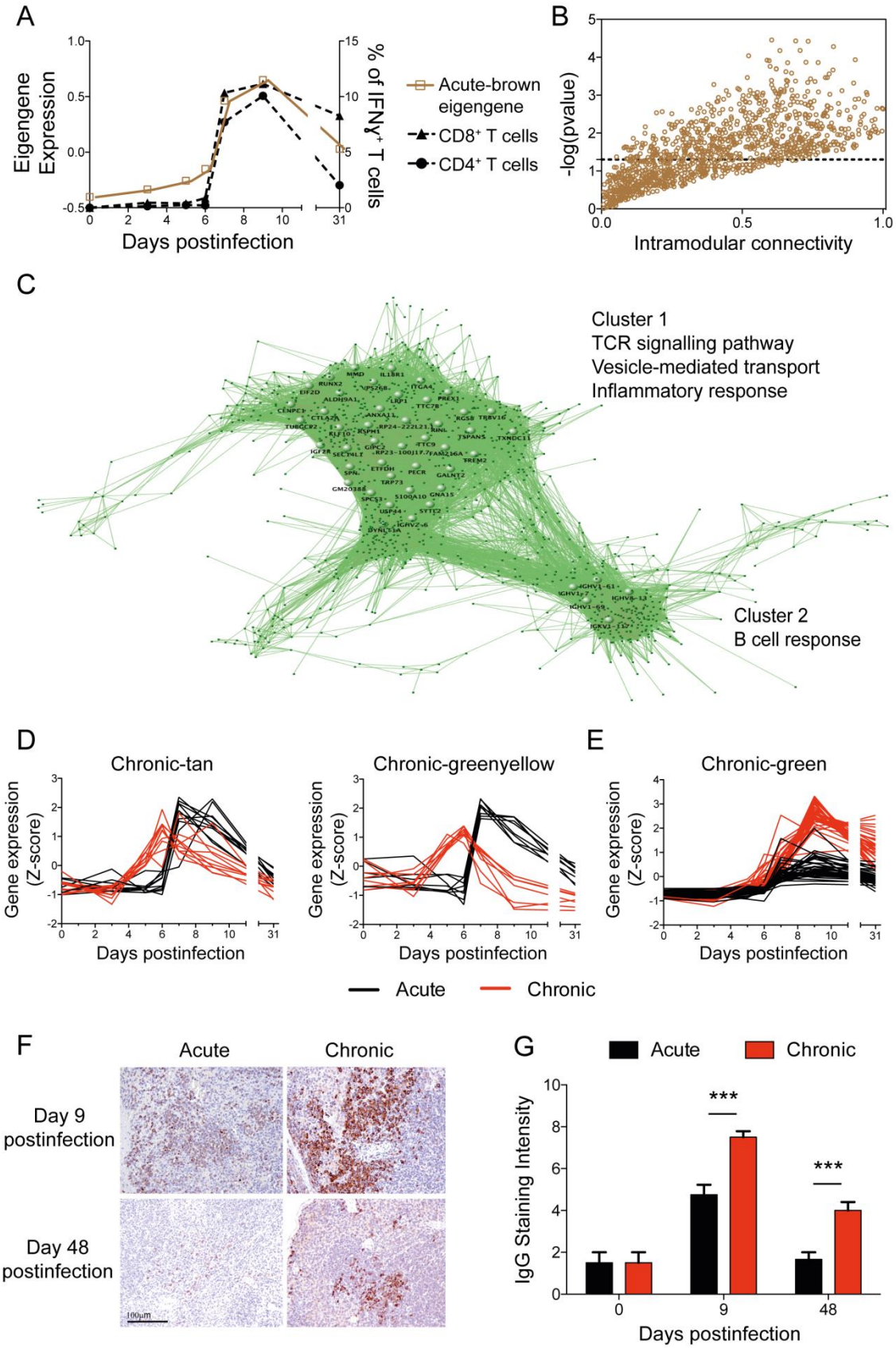
A
Eigengene Expression
% of IFNγ+ T cells
Days postinfection
Acute-brown eigengene
CD8+ T cells
CD4+ T cells
B
-log(pvalue)
Intramodular connectivity
C
Cluster 1
TCR signalling pathway
Vesicle-mediated transport
Inflammatory response
Cluster 2
B cell response
D
Chronic-tan
Chronic-greenyellow
Gene expression (Z-score)
Days postinfection
E
Chronic-green
Acute
Chronic
F
Acute
Chronic
Day 9 postinfection
Day 48 postinfection
100μm
G
IgG Staining Intensity
***
***
Days postinfection

3. Transcriptional network preservation between acute and chronic infections

The obtained gene coexpression modules represent the biological processes participating in acute and chronic infections. In order to identify the common and the specific features for both infection fates, we first determined the gene overlap between the acute and chronic modules by Fisher's Exact Test (Figure S3A). Eight acute and twelve chronic modules showed a high degree of overlap (pvalue<10^{-35}) with modules from the other group, and therefore they represent biological pathways that participate in both, acute and chronic infections. To then quantify module preservation (the degree to which coexpressed genes in acute infection are also coexpressed in chronic infection), we computed a connectivity-based preservation-statistic (Z-summary) that allows scoring the degree of similarity of the connectivity patterns between genes from two networks. Module preservation scores were inversely correlated with the percent of differentially connected genes (defined as those with a difference in their K_{IM} between acute and chronic networks higher than 0.4) (Figure R3A). This indicates that the preserved modules, that share similar gene connectivity patterns, also share common hub genes. Furthermore, module preservation scores correlated with the module size (Figure R3A), indicating that a large number of genes participate in biological pathways that are common in acute and chronic infection. In contrast, the biological pathways that are specific for an infection fate are governed by few genes.

To further examine the highly preserved modules, we compared their expression patterns (Figure S3B and S3C). Relevant overlapping hub genes between preserved modules are listed in Table S1. With the exception of the acute-yellow and the chronic-brown module that shared genes involved in type I interferon signaling (*Irf7*, *Mx1-2*, *Oas1a*, *Ifit1-3*), all the other highly preserved acute modules were decomposed into two modules in chronic infection. For instance, the acute-brown module overlapped with the chronic-green and the chronic-tan module, respectively, as described above (Figure R2). Interestingly, 36 hub genes from the acute-blue module overlapped with chronic-magenta, a module with a decrease in its expression between d7 and d9 when T cell exhaustion appears (Figure R1B). Four of these genes were related to neutrophil chemotaxis (*Itgb2*, *Itgam*, *Ccr1* and *C5ar1*). Their differential downregulation between acute and chronic infections at days 7 and 9 p.i. was confirmed in additional animals by qPCR (Figure S4A and S4B). A sustained expansion of neutrophilic MDSCs has been described in LCMV chronic infection (Norris et al. 2013). Therefore, these results suggest that prior to the appearance of neutrophilic MDSCs, there is an alteration in the migration of these cells concomitant with exhaustion of $CD8^+$ T cells.

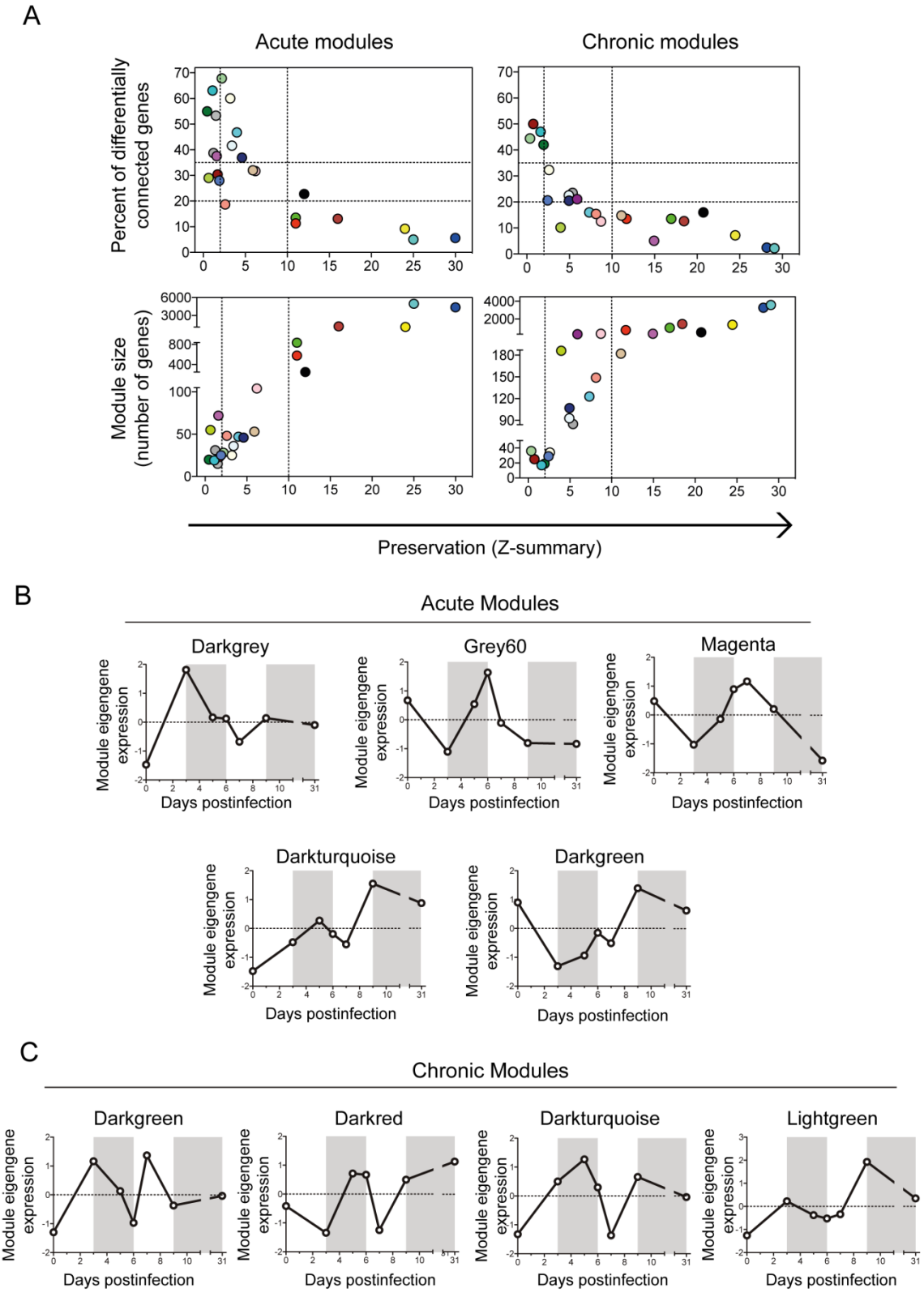

Figure R3. Module preservation between acute and chronic infections. (A) Module preservation scores were compared to the percent of differentially connected genes in a module and to module size. Dashed lines indicate the thresholds (see Supplemental Experimental Procedures for details). (B and C) Eigengene expression profiles of (B) acute- and (C) chronic-specific modules

The modules with low preservation scores represent biological processes specific of acute or chronic infections, and therefore might provide novel mechanisms influencing infection fates. We identified five acute-specific and four chronic-specific modules (Figure R3B and R3C). The respective genes and their connectivity values are listed in Table S2. Acute-specific modules showed diverse expression profiles characterized by marked expression peaks at different time points. The included genes represent both innate and adaptive immune pathways highlighting the need of diverse biological responses to properly resolve a viral infection. On the other hand, all chronic infection-specific modules showed expression changes between days 7 and 9 p.i., when T cell exhaustion appears (Figure R3C), thus indicating that critical events governing chronic infection fates occur in this time window. Group-specific modules are further analyzed in the next sections.

4. Early attenuation of the inflammatory response in chronic infection

Acute infection-specific modules are expected to participate in the resolution of the virus infection. From the 5 acute-specific modules (Figure R3A), the acute-grey60 module was most interesting. It has a marked expression peak at day 6 postinfection (Figure R3B) just before the specific T cell response appeared thus bridging innate immune responses with the adaptive response. All 31 genes of this module are highly coexpressed only during acute infection (Figure R4A) and enriched for genes involved in the regulation of IL6 and IL12 production (Figure R4B). As IL6 and IL12 are pro-inflammatory cytokines with important roles in antiviral host responses, our observations suggested a differential regulation in both infection fates before T cell exhaustion becomes apparent. To verify this hypothesis, we plotted the *Il6* and *Il12b* expression kinetics from our RNA-seq data (Figure R4C) and validated the IL6 expression results by qPCR including additional infected animals. Both, RNA-seq and qPCR gave consistent results showing a peak of IL6 expression at d6 after acute infection that was lacking in chronic infection (Figures S4C). Since inflammatory responses are complex responses, we next sought to identify whether *Il6* and *Il12* were part of a broader cluster of coexpressed genes within their acute-blue module. Indeed, we found 1504 genes in acute-blue module to correlate to the *Il6* expression kinetics with a correlation value above 0.8. Moreover, the level of expression of 79 of these genes was significantly higher in acute than in chronic infection at d6 p.i. (log2FC>1) (Figure R4D). A list of 27 representative genes from this submodule, and their expression profiles in acute and chronic infections is shown in figures R4E and R4F, respectively.

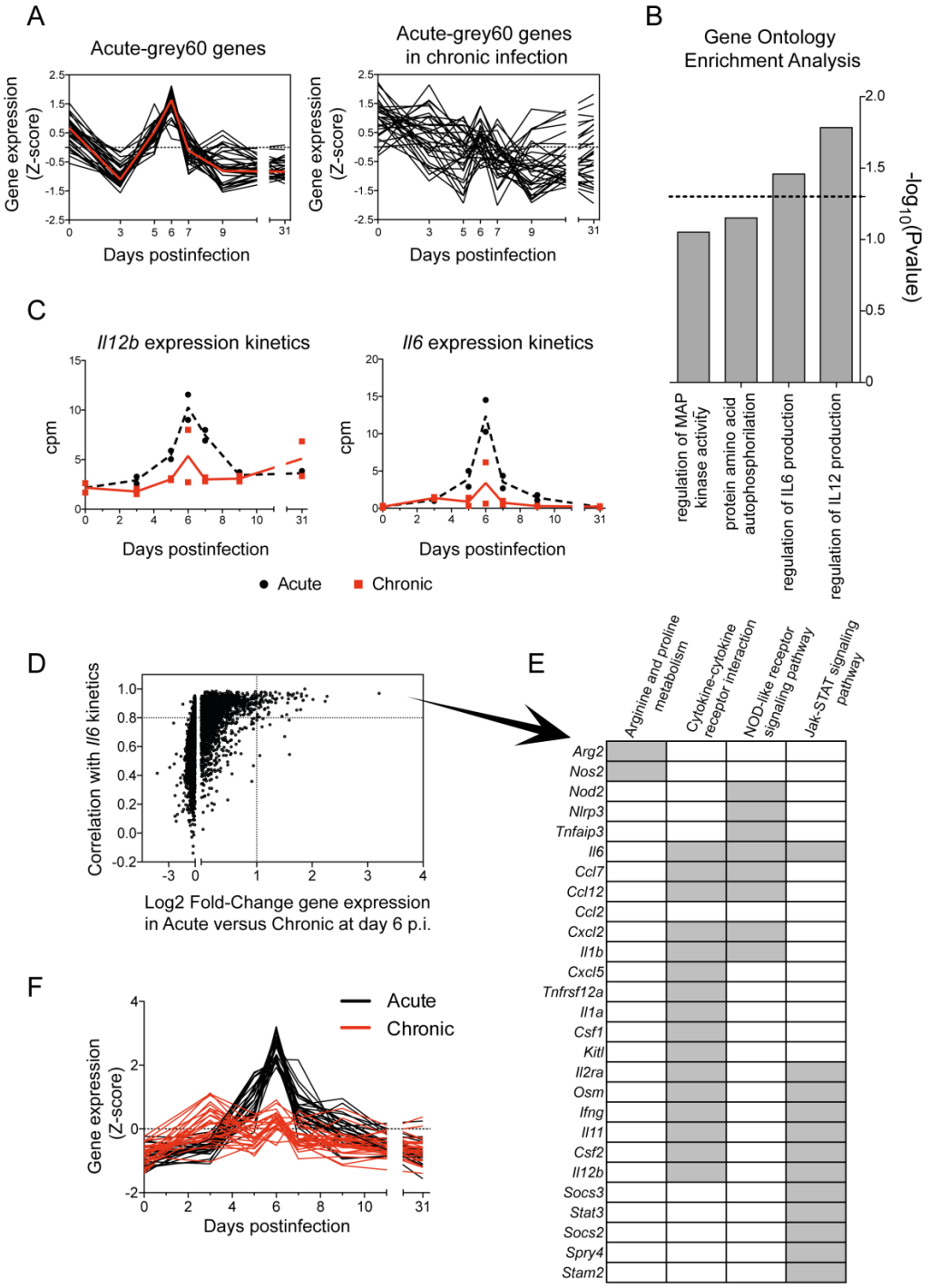

Figure R4. Acute-grey60-specific module has a differential regulation of genes related to macrophage inflammatory response. (A) Normalized expression kinetics of genes from the acute-grey60 module and their kinetics in acute infection. Red line represents the eigengene. (B) GO terms enriched in genes from the acute-grey60 module (dashed line marks p=0.05). (C) RNA-seq-derived *Il12b* and *Il6* expression kinetics. (D) Pearson's correlation between genes of the acute-blue module and *Il6* in acute infection is plotted against the log2 fold-change (log2FC) of gene expression between acute and chronic infection at day 6 p.i.. Dashed lines mark a correlation >0.8 and log2FC>1. (E) List of 27 representative genes with a correlation>0.8 with *Il6* expression kinetics, and log2FC>1 of gene expression between acute and chronic infection at day 6 p.i.. Grey boxes indicate the enriched KEGG pathways that each gene belongs to. (F) Normalized expression kinetics of the 27 genes.

KEGG pathway analysis showed enrichment of genes involved in inflammatory pathways such as the NOD-like receptor and the Jak-STAT signaling pathways, and cytokine-cytokine receptor interaction. Moreover, we identified two genes related to the metabolism of Arginine and Proline (*Arg2* and *Nos2*), a pathway known to play an important role in the regulation of inflammation by monocytes and macrophages (Burrack & Morrison 2014). Il1b and Nos2 expression kinetics was further confirmed by qPCR including additional infected mice (Figure S4C). Together these data show differential spleen monocyte/macrophage characteristics during early time points of acute and chronic virus infections.

To test the hypothesis of an early differential polarization of monocyte/macrophages during both outcomes of LCMV infection, we characterized spleen monocyte/macrophages at day 6 postinfection by intracellular IL6 staining and RNA-seq. The percentage of IL6-producing monocytes/macrophages from chronic infection were significantly lower than those from acute infection while the number of pro-inflammatory Ly6C^{hi} monocytes/macrophages in the spleen were, as described before (Norris et al. 2013), similar in both infections (Figure R5A). Transcriptional profiling from sorted monocytes/macrophages showed that cells from acute infection expressed higher levels of pro-inflammatory cytokines and chemokines, and cellular receptors and transcription factors associated to M1 macrophages. In contrast, monocytes/macrophages from chronic infection expressed higher levels of transcription factors and genes that exert anti-inflammatory effects and markers of M2 macrophage differentiation (Figure R5B). These data demonstrate that inflammatory monocytes/macrophages are induced early after an acute LCMV infection and, in contrast, during chronic infection these cells shift to an anti-inflammatory profile before T cell exhaustion becomes evident. Importantly, the monocytic cell population of chronic infection had an upregulated expression of genes involved in arachidonic acid secretion such as *Pla2g2d* (phospholipase A2 group IID), an anti-inflammatory lipid mediator (Miki et al. 2013). Since these molecules play an important role in the resolution of inflammation (Sugimoto et al. 2016), one might expect a tissue protective role of these cells in chronic infection. To test this idea, we quantified the level of fibrosis in spleens from acute and chronic LCMV infections by Masson's trichrome staining. Fibrosis, a feature of insufficient resolution of chronic inflammation, was evident as early as d10 in acute infection, and remained elevated even at days 15 and 48, when the virus infection is resolved (Figure R5C and R5D). In contrast, fibrosis was only observed in chronic infection in one of 4 animals at d48. Together this suggests that besides the known role of suppressive monocytic cells to dampen virus T cell responses in chronic infection, they also might participate in inflammation resolution via expression of pro-resolving lipid mediators that finally lead to fibrosis prevention.

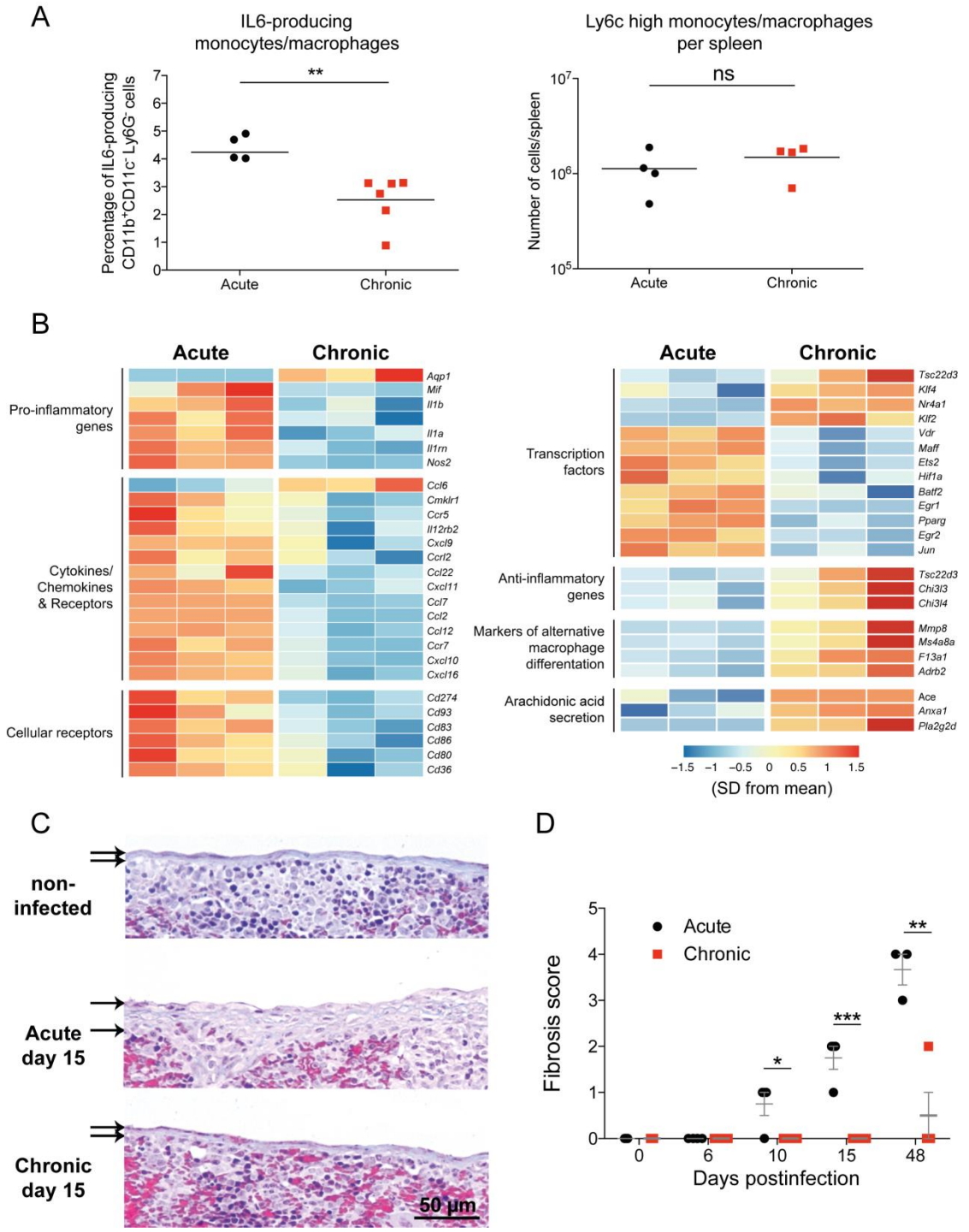

Figure R5. Early shift from inflammatory to pro-resolving monocytes/macrophages in chronic infection to prevent fibrosis. (A) Percentage of IL6-producing CD11b^{+} CD11c^{-} Ly6G^{-} cells and number of Ly6Chi monocytes/macrophages per spleen at day 6 pi. (B) Heatmap illustrating the relative expression of genes in monocyte/macrophage cells from acute and chronic infected mice at day 6 p.i.. (C) Representative images of Masson's trichrome staining of spleens. Thickness of the splenic capsules are marked by arrows. Magnification bar: 50µm. (D) Semiquantification of fibrosis in spleens. Data shown are mean ± SEM of n=4 to 5 mice. * $p \leq 0.05$; ** $p \leq 0.01$; *** $p \leq 0.001$ (unpaired two-tailed t test).

5. The XCL1-XCR1 communication axis links T cell exhaustion with effector cell maintenance

Cytokines and chemokines are major components of the signalling network that regulates the coordinated immune response against a viral infection (Cameron & Kelvin 2003). Thus, we next investigated which cytokines/chemokines-encoding hub genes were present in acute- and chronic-specific modules, and therefore might participate in processes involved in infection fate regulation. From all the identified hub genes (Table S2), of particular interest was the chemokine-encoding gene *Xcl1* from the chronic-darkturquoise module. XCL1 is mainly produced by NK and activated $CD8^+$ T cells, and promotes the recruitment of dendritic cells expressing the receptor XCR1 ($XCR1^+$ DCs) which are implicated in the priming and boosting of cytotoxic responses to cross-presented antigens(Kroczek & Henn 2012).

All 17 genes of the chronic-darkturquoise module are highly coexpressed in chronic infection and deregulated in acute infection (Figure R6A). They show a "two-peak" behaviour with an expression peak at d5 and a second upregulation from d7 to d9 p.i.. The second peak of expression of XCL1 was verified by qPCR using additional infected mice (Figure S5A). In contrast to chronic infection, *Xcl1* showed only a single early peak of expression at d6 in acute infection, returning to basal levels from d7 p.i. (Figure R6B). To investigate the role of XCL1 during the establishment of the chronic infection phase, we first analyzed the chemokine expression by NK and $CD8^+$ T cells at d9 by intracellular staining. Both NK and $CD8^+$ T cells showed a higher expression of XCL1 in chronic infection compared to acute infection or uninfected mice (Figure R6C). Importantly, XCL1 was highly produced by LCMV-specific $CD8^+$ T cells once exhaustion was established (Figure R6D and S5B), and particularly abundant in the subpopulation of $CXCR5^+$ cells (Figure R6D). As virus-specific $CXCR5^+$ $CD8^+$ T cells have recently been shown to play a major role in the control of virus replication during chronic infections (Im et al. 2016; He et al. 2016), our data now show that they also play an important role in the immune adaptation process during exhaustion.

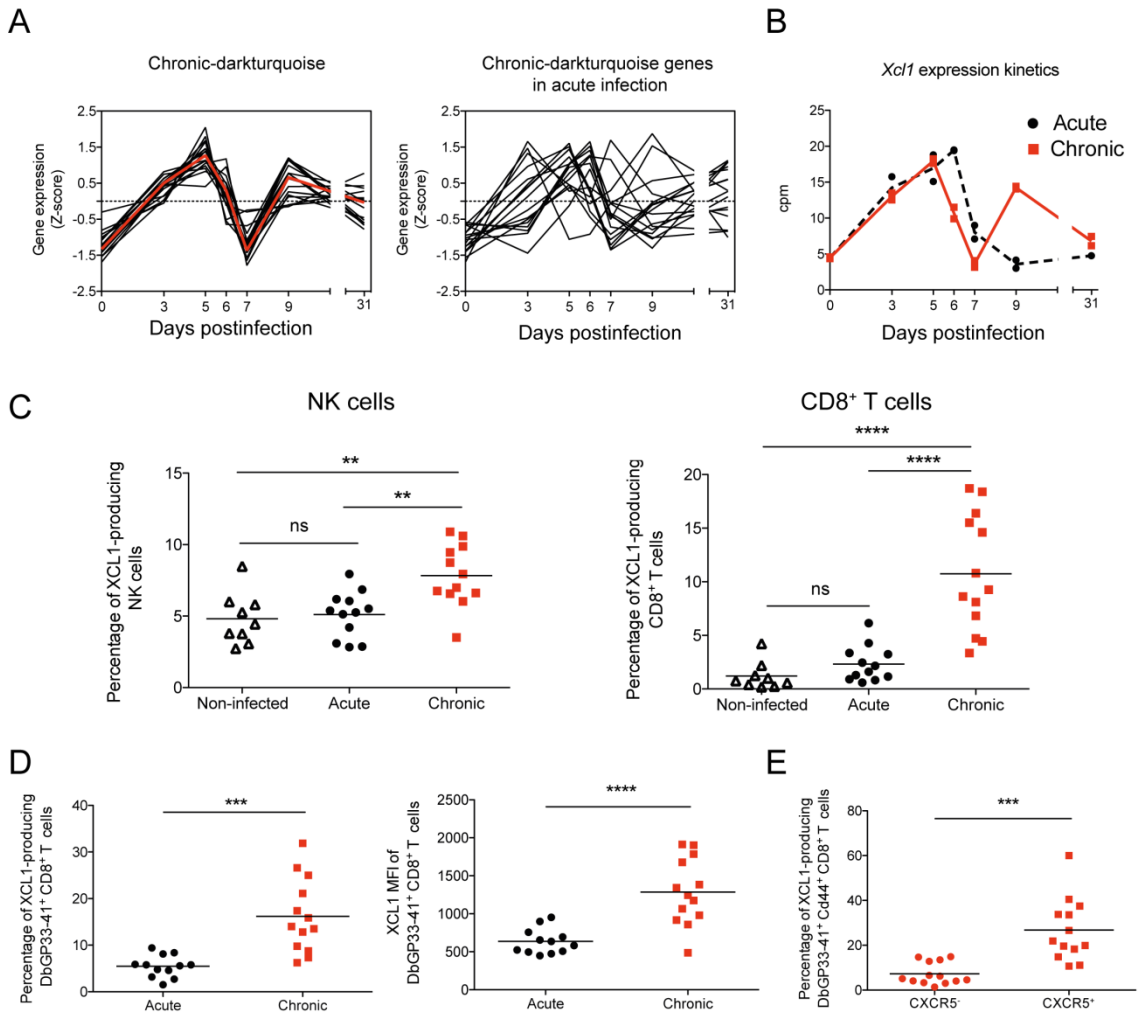

Figure R6. Chronic-darkturquoise specific module reveals an important role of XCL1 in chronic infection. (A) Normalized expression kinetics of genes from the chronic-darkturquoise module and their corresponding kinetics behaviour in acute infection. (B) Xcl1 expression kinetics obtained from the RNA-seq analysis. (C) Percentages of XLC1-producing NK and CD8+ T cells at day 9 p.i. Data shown are mean ± SEM from n= 11 to 13 mice representative of three independent experiments (significance determined using one-way ANOVA). (D-E) MFI of XLC1 in DbGP33-41+ CD8+ T cells (D) and percentages of XLC1-producing DbGP33-41+ CD8+ T cells (D) and CXCR5- or CXCR5+ DbGP33-41+ CD44+ CD8+ T cells (E) at day 9 p.i.. Data shown are mean ± SEM from n= 11 to 13 mice (significance determined using unpaired two-tailed t test). ns, not significant; ** $p \leq 0.01$; *** $p \leq 0.001$; **** $p \leq 0.0001$.

Coinciding with the second peak of XCL1 expression, the quantification of XCR1$^+$ DCs showed a clear increase of these cells in the spleens at d9 in chronic infection (Figure R7A and S5C). To further analyze the impact of this XCL1-XCR1 axis, we depleted XCR1$^+$ DC in chronically-infected XCR1-DTRvenus mice (Yamazaki et al. 2013b) with diphtheria toxin (DT) (Figures R7B and S5D). While the virus-specific CD4$^+$ T cell response was not affected, XCR1$^+$ DC depletion led to a significant reduction in the percentage of GP33-specific CD8$^+$ T cells at day 15 p.i. and lower percentages of CD107a, CD107b and IFN-γ producing cells than in untreated animals (Figure R7C). Moreover, the percentage of

CXCR5$^+$ CD8$^+$ T cells was also significantly decreased suggesting an interdependence between this CD8$^+$ T cell subset and cross-presenting XCR1$^+$ DCs. Consistently, the viral titers in spleen, lung and kidney were higher in mice lacking XCR1$^+$ DCs (Figure R7D). Together these results demonstrate that the XCL1-XCR1 communication axis is (i) an important component of immune system adaptation to an overwhelming virus threat and (ii) an important component of virus control in the chronic infection phase.

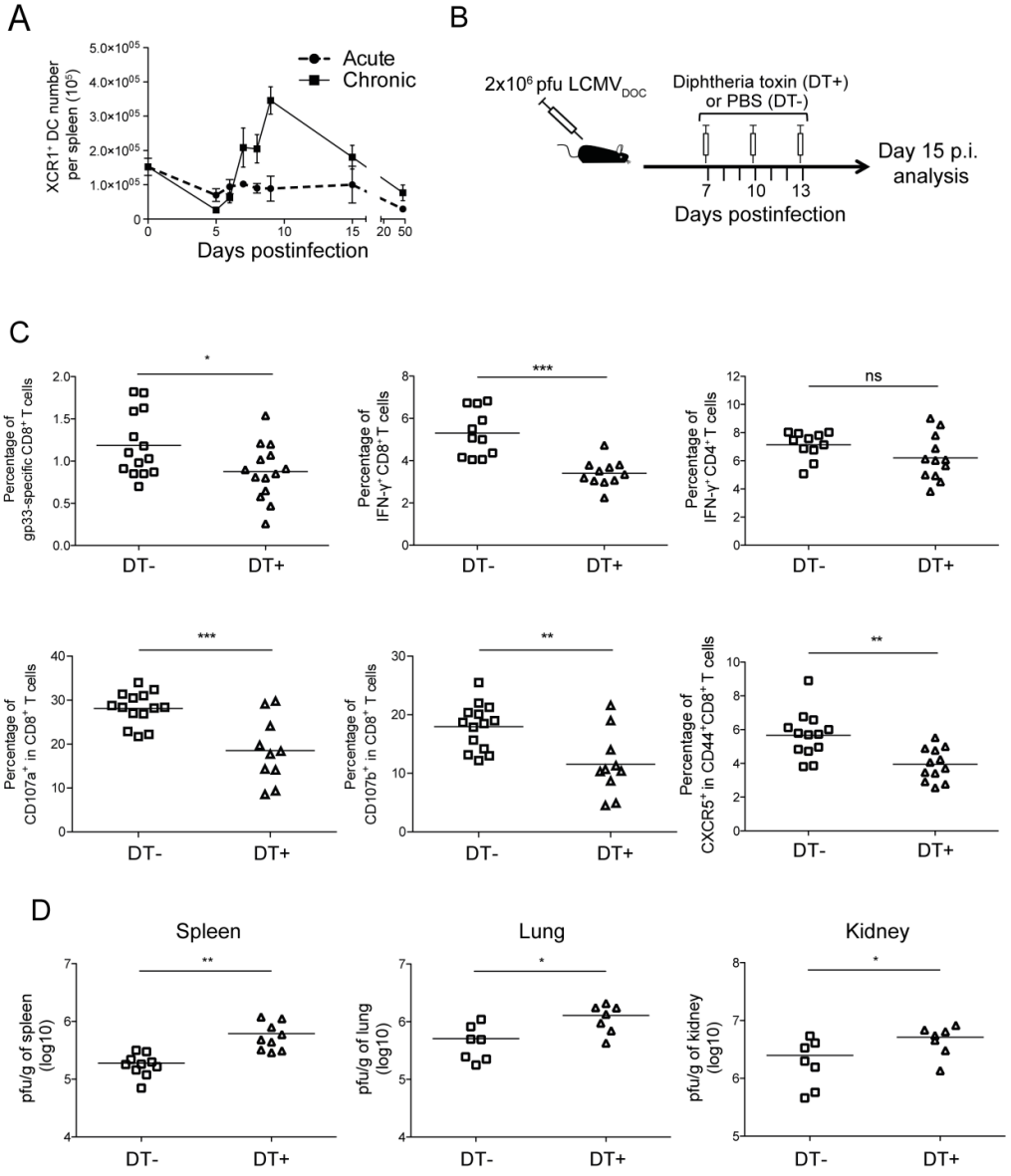

Figure R7. XCR1+ dendritic cells are required to maintain antiviral T cell response and control virus titers (A) Number of XCR1+ dendritic cells in spleen. (B) Schematic representation of DT treatment regimen for depletion of XCR1+ dendritic cells. (C) Percentages of DbGP33-41+ CD8+ T cells, IFN-γ-producing CD8+ and CD4+ T cells, CD107a+ and CD107b+ CD8 T cells, and CXCR5+ CD44+ CD8+ T cells from chronic infected mice non treated (DT-) or treated (DT+) with DT at day 15 p.i.. (D) Virus titers in spleen, lung and kidney from chronic infected mice non treated (DT-) or treated (DT+) with DT at day 15 p.i.. (C-D) For each group replicates and the mean ± SEM is shown. ns, non significant; * $p \leq 0.05$; ** $p \leq 0.001$; *** $p \leq 0.0001$ (unpaired two-tailed t test). Data are representative of two or three independent experiments.

SUPPLEMENTAL FIGURES AND TABLES

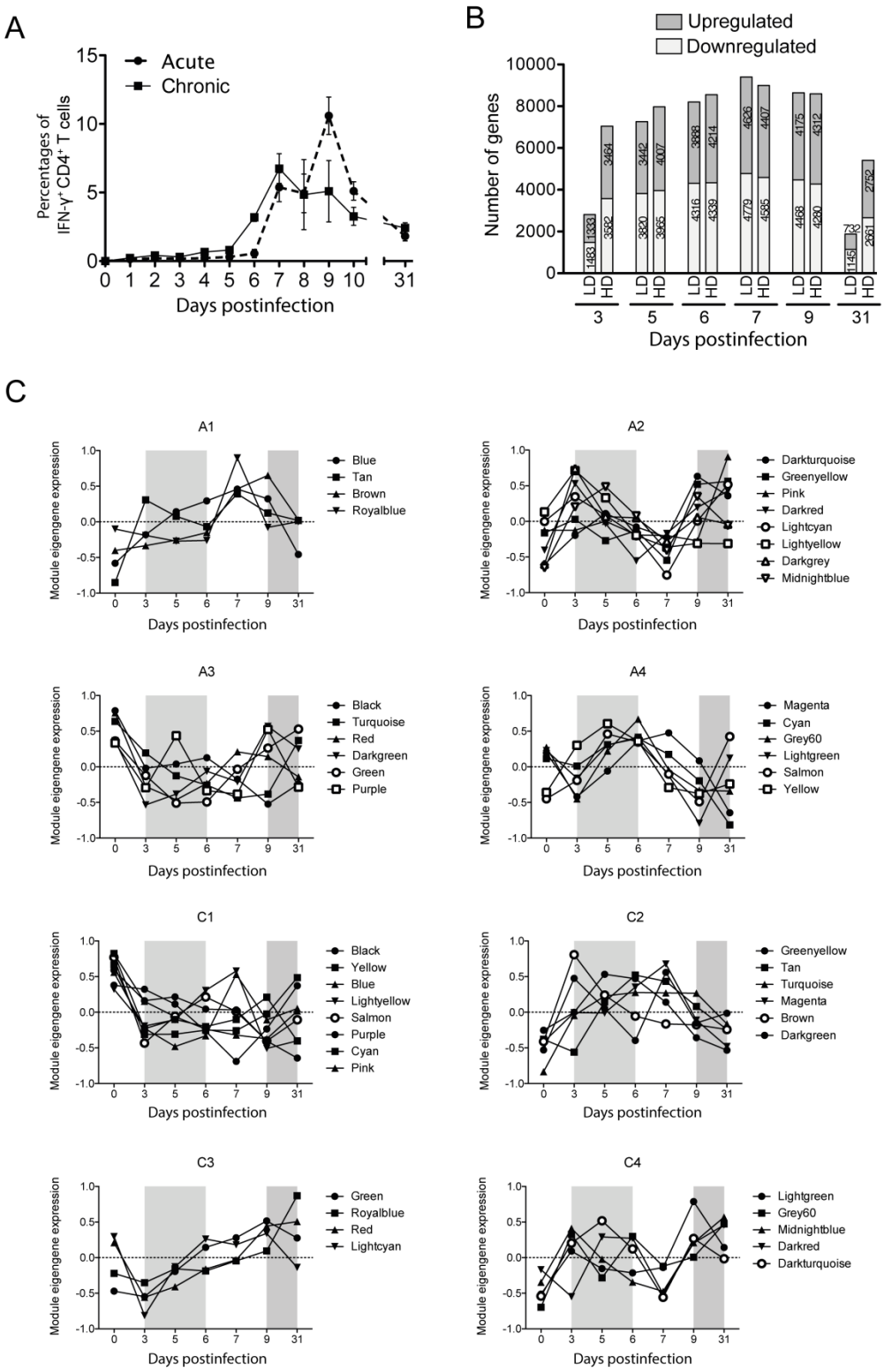

Figure S1. Kinetics of CD4$^+$ T cell response, analysis of differentially expressed genes and module eigengene expression patterns. (A) Percentages of IFN-γ-producing CD4$^+$ T cells were determined by ICS after stimulation with GP61. For each group and time point, the mean ± SEM is shown. (B) Differentially expressed genes in spleens after LCMV infections. Number of differentially expressed genes that were up- or down-regulated after infection were calculated for each time point. (C) Module eigengene kinetics grouped based on hierarchical clustering obtained from acute (A) and chronic (C) infections.

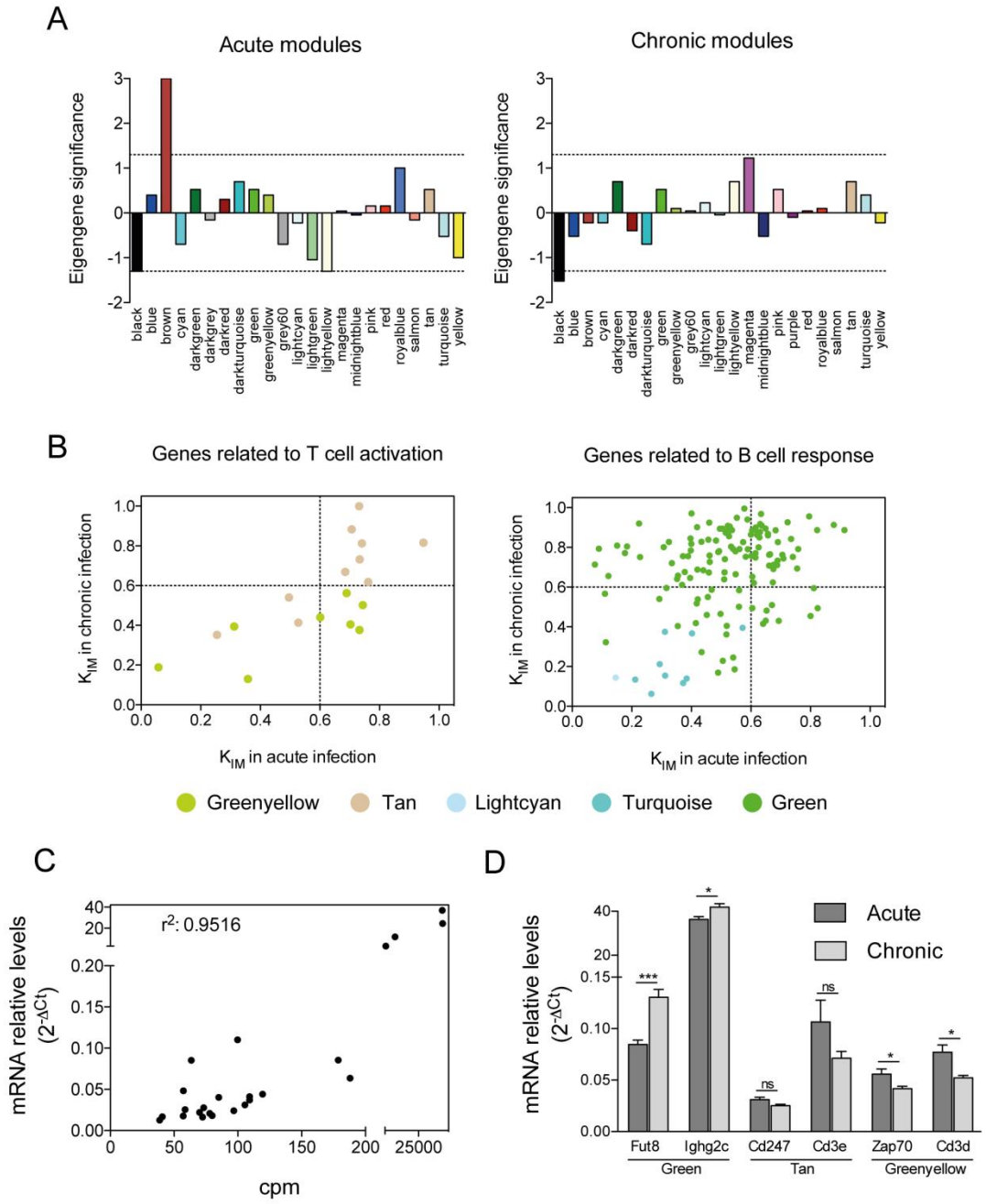

Figure S2. Acute-brown module represents T and B cell responses in acute infection. Related to Figure R2. (A) Bar plot of eigengene significances indicating the correlation (Pearson) of each module with virus-specific IFN-γ-secreting CD8$^+$ T cell kinetics (-log(pvalue); modules with negative correlation are plotted with a negative value). (B) Intramodular connectivity (K_{IM}) of genes related to T and B cell responses from the acute-brown module. Each gene is labeled by the corresponding module color of the chronic infection. Genes related to T cell activation are *Spn*, *Cd247*, *Cd3e*, *Cd3d*, *Themis*, *Prkcq*, *Zap70*, *Trbc1*, *Thy1*, *Grb7*, and the transcription factors *Maf* and *Nfatc2*; representative genes related to B cell response are *Fut8*, *Ighv*, *Iglv*, *Igkv*, *Igkc*, *Ighg*, *Ighj*, *Cdkn2c*, and *Cdk6*. (C-D) Expression levels at d9 p.i. of six genes related to T and B cell responses from acute-brown module were measured by qPCR and correlated to the expression values obtained by RNAseq (C), and validated with more animals (D; 6 to 8 mice/group; in X-axis are shown gene names and their respective module in chronic infection). Unpaired two-tailed t test. ns, non significant; * $p \leq 0.05$; *** $p \leq 0.001$.

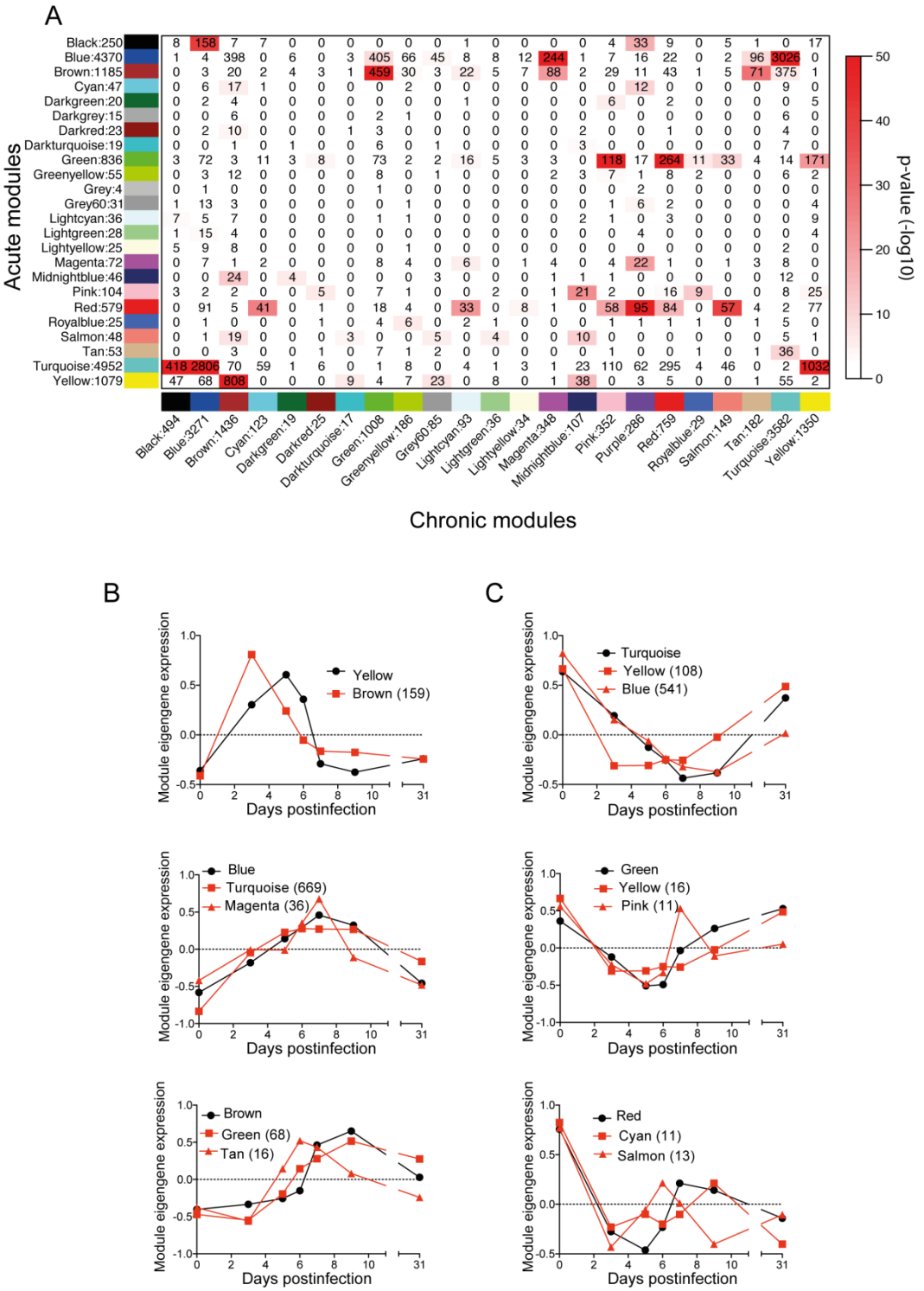

Figure S3. Gene overlapping and expression kinetics of highly preserved modules. (A) Heatmap of module gene overlapping between infections. Each row and column is labeled by the corresponding module color, and the total number of genes in the module. Numbers within the table represents the number of genes in common between the corresponding modules. The significance of gene overlap was calculated by Fisher's exact test. Pvalues are color coded according to the color bar on the right. (B and C) Eigengene expression profiles of highly preserved modules between acute (red) and chronic (black) infections containing genes upregulated (B) or downregulated (C) after infection. The number of overlapping hub genes between the corresponding chronic and acute modules are indicated in brackets.

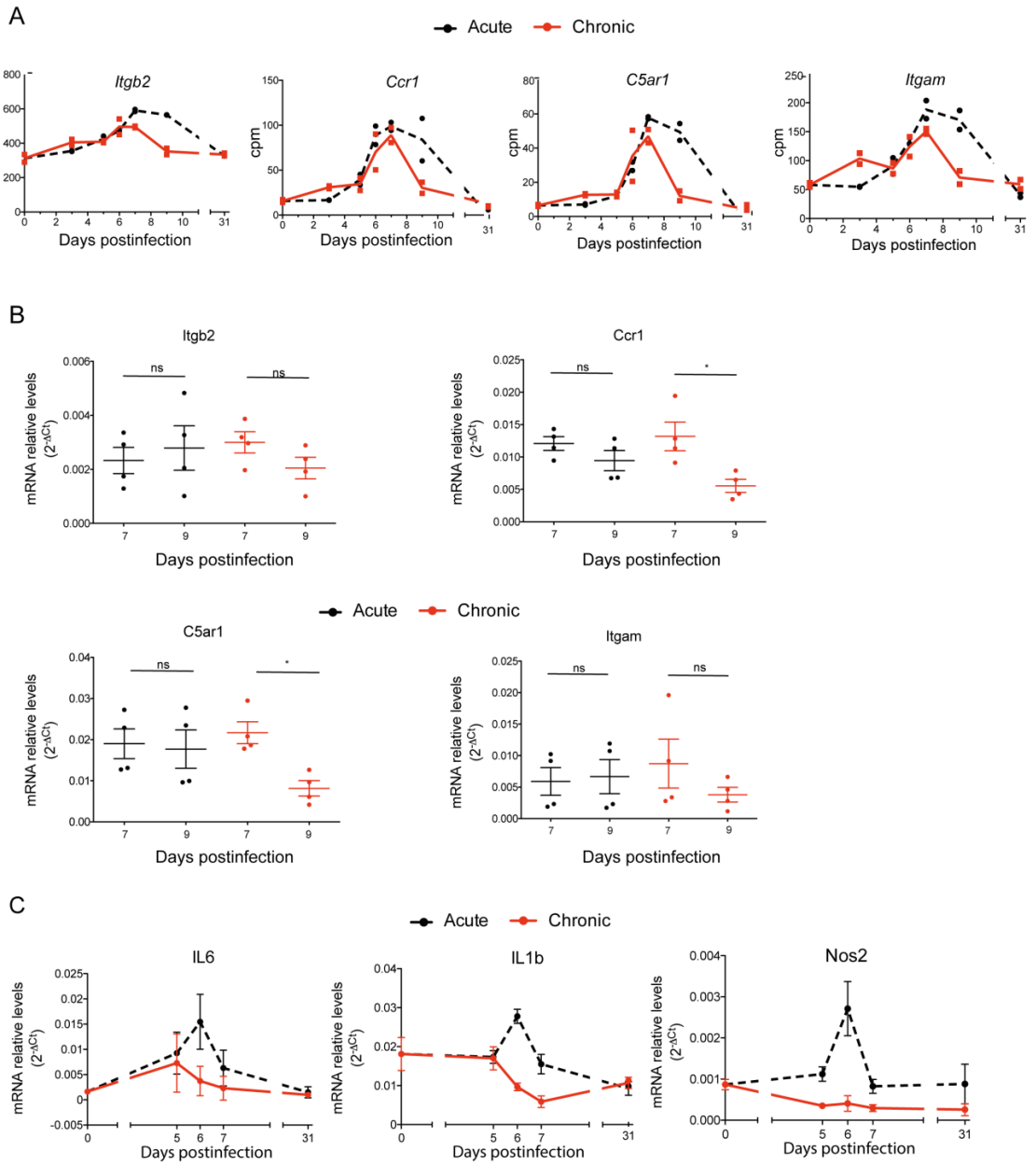

Figure S4. Validation of RNAseq-derived gene expression by qPCR and analysis of monocytes/macrophages. Related to Table S1 and Figure 4. (A) Normalized gene expression (cpm) kinetics obtained from RNAseq analysis of the spleens of acute and chronic infected mice. (B-C) Quantitative PCR of the leukocyte chemotaxis related genes *Itgb2*, *Ccr1*, *C5ar1* and *Itgam* (B), and *Nos2*, *IL1b* and *Il6* (C) was performed at the indicated days postinfection from spleens of acute and chronic infected mice. Relative gene expression level was normalized by GAPDH. Data are shown as mean ± SEM from 5 to 6 mice. Significant differences were determined by an unpaired two-tailed t test. ns, non significant; * $p \leq 0.05$; ** $p \leq 0.01$.

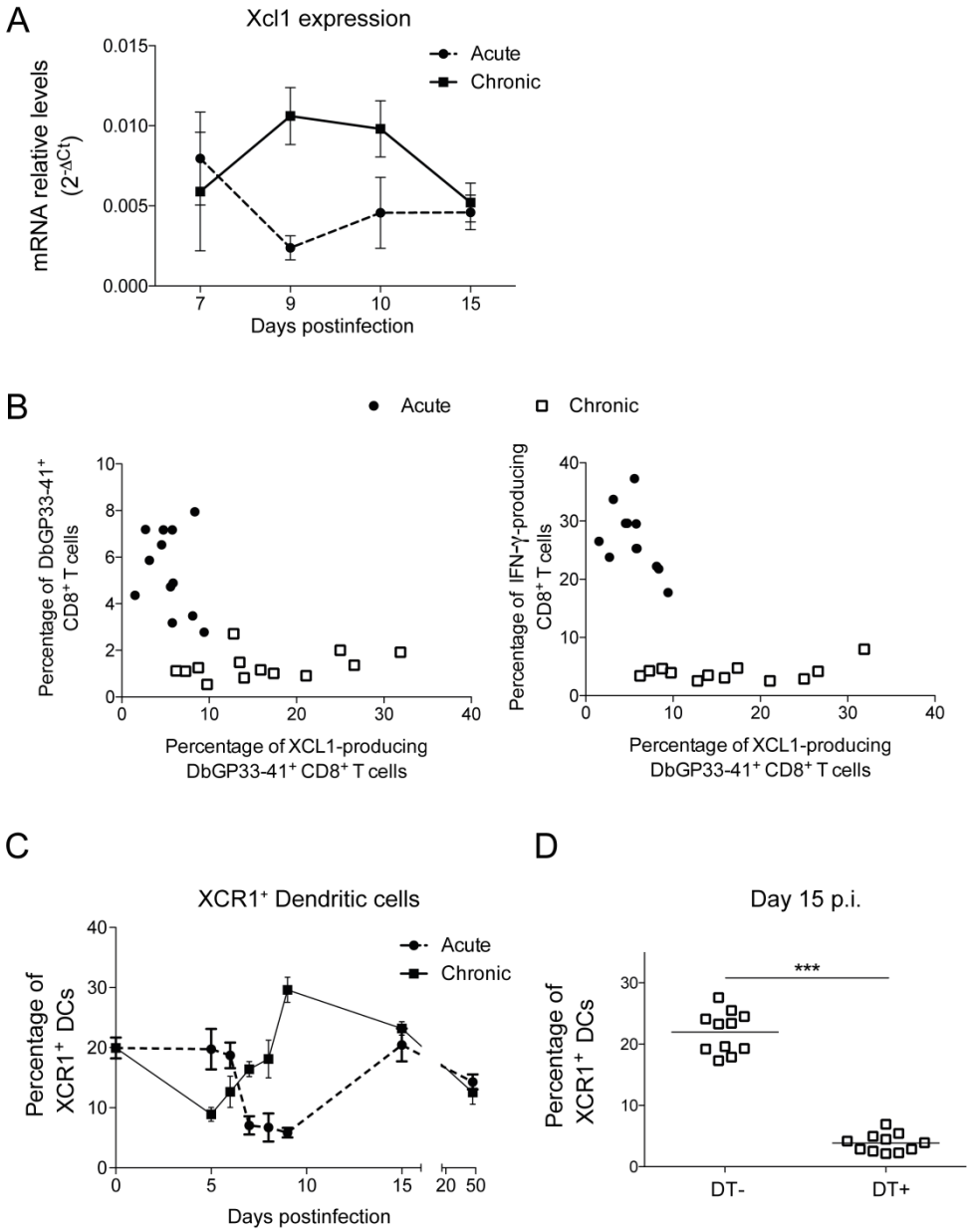

Figure S5. Analysis of Xcl1 expression and quantification of XCR1$^+$ DCs. (A) Quantitative PCR of Xcl1 was performed at the indicated days postinfection from spleens of acute and chronic infected mice. Relative gene expression level was normalized by GAPDH. For each group and time point, the mean ± SEM is shown. (B) Percentage of XCL1-producing DbGP33-41$^+$ CD8$^+$ T cells is plotted against the percentage of DbGP33-41$^+$ CD8$^+$ T cells and IFN-γ-producing CD8$^+$ T cells. (C) Percentage of XCR1$^+$ dendritic cells in spleen over the course of the infection in acute or chronic infected mice determined by flow cytometry analysis. (D) Spleen lymphocytes were harvested at day 15 postinfection from chronic infected mice non treated (DT-) or treated (DT+) with Diphtheria Toxin and percentages of XCR1$^+$ dendritic cells were assessed. Data are representative of three independent experiments. For each group the mean ± SEM of n= 11 is shown. *** $p \leq 0.001$ (Unpaired two-tailed t test).

Table Supplementary 1. Overlapping hub genes between preserved modules. When the number of overlapping genes>100, only genes representing relevant biological functions obtained from David are shown.

Acute Yellow	# Overlapping genes: 159	Chronic Brown
Innate immune response *Oas3, Bst2, Mx2, Herc6, Zbp1, Ddx58, Oas1a, Ifit2, Pml, Ifih1, Ripk2, Mx1, Ifitm3, Samhd1, Oasl1, Rnf135, Ifit3, Irf7, Trim21, Dhx58, Ifit1* Cellular response to interferon-alpha *I830012O16Rik, Ifit3, Myc, Ifit2, Ifit1* Cellular response to interferon-beta *Trex1, Ifit3, Ifi205, Ifit1* Antigen processing and presentation of peptide antigen via MHC class I *H2-T22, H2-Q4, H2-M3, H2-T23, H2-Q6, H2-Q7, H2-K1, H2-T10*		

Acute Turquoise	# Overlapping genes: 108	Chronic Yellow
Regulation of transcription, DNA-templated *Rfx7, Zfp62, Purb, Suv420h1, Zfp81, Zscan26, Ubp1, Zfp68, Pura, Zfp560, Zfp317, Zfp770, Txlng, Rnf38, Gm12258, Ehf, Pou2f1* Positive regulation of GTPase activity *Gm13304, Rapgef6, Dennd6a, Ccl21a, Gm21541* Lymphocyte chemotaxis *Gm13304, Ccl21a, Gm21541*		

Acute Turquoise	# Overlapping genes: 541	Chronic Blue
Regulation of transcription, DNA-templated *Crtc1, Jarid2, Zfp764, Zscan2, Sap25, Brd3, Kdm5b, Mapk11, Zfp318, Asxl3, Zfp688, Zfp579, Il16, Gm9897, Zfp932, Zfp943, Ring1, Arid3b, Brwd1, Wasl, Zbtb9, Zfp866, Gpbp1l1, Zfp740, Foxp1, Krba1, Zbtb49, Ebf4, Hes5, Phf1, Smad7, Rfx1, Prdm11, Akap8l, Zfp420, Cux1, Zfp653, AW146154, Zfp867, Crebzf, Ebf1, Srsf5, Sp6, Cbx7, Gm15446, Mterfd2, Crtc3, Hmg20a, Zfp942, Rarg, Foxj3, Kdm3b, Epc1, Cdkn2aip, Hes6, Zfp212, Ezh1, Ccnt2, Kdm4b, Chd6, E4f1, Ccar2, Hif1an, Arid4b, Camta1, 5830428H23Rik, Foxj2, Nfe2l3, Zfp512, Ddx5, Per3, Meis1, Phf21a, Sirt7, Zfp182, Dbp, Zfp592, Tle2, Zmym5, Dmtf1, Mterf, Nfrkb, Zfp275, Zfp746, Zscan20, Fam120b, Irf3, Hdac10, Akap8, Tspyl2, Zfp956, Prdm9, Lrif1, Mterfd3* Covalent chromatin modification *Jarid2, Phf21a, Hmg20a, Brd3, Ing4, Sirt7, Kdm5b, Phf1, Kdm3b, Epc1, Ring1, Ogt, Hdac10, Ezh1, Tspyl2, Chd6, Kdm4b, Msl1, Cbx7, Prdm9* Protein phosphorylation *Map2k7, Sbk1, Obscn, Ulk3, Stk11, Phkg2, Map3k1, Mapk11, Ikbkb, Clk4, Prkcg, Map4k2, Clk1, Mast3, Nek8, Tec, Pan3, Clk2, Map4k1, Ltk, Fgfr3, Npr2, Csnk1g2*		

Acute Blue	# Overlapping genes: 669	Chronic Turquoise
Cell cycle *Tipin, Ran, Uhrf1, Clspn, Kif2c, Zwilch, Mastl, Gm6531, Ska3, Suv39h1, Ckap2, Cks2, Gmnn, Mybl2, Cdc20, Aurka, Cenpw, Cdc34, Cdca8, Nuf2, Cdk4, Psrc1, E2f7, Mcm8, Ercc6l, Pin1, Cinp, Rbbp8, Ncaph, Mcm4, Ccnb1, Mcm6, Chaf1a, Erh, Cdc123, Cdc25a, Bub1b, Mad2l1, Gsg2, Cep55, Nasp, Ube2s, Spdl1, Cdca2, Cdk1, Spc24, Dbf4, Nup37, Tfdp1, Tpx2, Lig1, Cdca5, Plk1, Cks1b, Mcm2, Bub1, Aurkb, Ppm1g, Hells, Ticrr, Chaf1b, Mcm5, Mcm3, Cdc45, Melk, Nek2, Bub3*		

Acute Blue	# Overlapping genes: 36	Chronic Magenta
Itgb2, Lcp2, Por, Kctd5, Fos, Slc7a8, Adamts1, Slc16a3, Ccr1, Slc11a1, Tagln2, Soat1, Rbms1, Plin2, Ptpn12, Itgam, F7, Pkm, Pdcd6ip, Alas1, Atp1a1, Rnpep, Hilpda, D630023F18Rik, C5ar1, Rnd1, Gm15590, Aldoart1, Atp8b4, Gm12164, Gm13365, Mrgpra2a, Gm13812, Gm13810, Mrgpra2b, E230013L22Rik		
Acute Green	**# Overlapping genes: 16**	**Chronic Yellow**
Unc5b, Cacna1g, Kat6b, Slc12a2, Dcaf12, Gm996, 2410066E13Rik, Zfhx3, Pitpnc1, Foxo4, A830010M20Rik, B230219D22Rik, Mmp12, Sox4, Zfp433, Gm26702		

Acute Brown	# Overlapping genes: 16	Chronic Tan
Cd247, Grb7, Fam71b, Prkch, Tmem180, Tubgcp2, Cd3e, Gipc2, Kremen2, Themis, Spn, Trbv14, Trbv29, Zan, B930095G15Rik, 4930519F09Rik		

Acute Green	# Overlapping genes: 11	Chronic Pink
Trpv4, Abcc3, Acot2, Fam168a, Mgll, Tie1, Decr2, Snrk, Fndc4, Fam211b, Tmem19		

Acute Red	# Overlapping genes: 13	Chronic Salmon
Dip2a, Abca2, Tnik, 2610020H08Rik, Xlr4c, Galnt6, Cep250, Yeats2, Kif21b, Usp48, Lsm11, Xlr4b, Tmppe		

Table S2. Chronic-specific module gene list. (*genes regulated by Klf4).

Acute_Magenta		Acute_Magenta (cont)		Acute_Grey60		Chronic_Lightgreen	
Gene	K_{IM}	Gene	K_{IM}	Gene	K_{IM}	Gene	K_{IM}
Adgb	1.000	*Pkd1l3*	0.412	*Nufip2*	1.000	*Gm11747*	1
Serpina3b	0.978	*1700034H15Rik*	0.403	*Lilra6*	0.930	*Dtwd1*	0.982
Car12	0.947	*Wdr19*	0.388	*Slc39a2*	0.870	*C1qtnf1*	0.857
Stk35	0.933	*Grtp1*	0.358	*Camsap1*	0.859	*Fam83g*	0.819
Myo19	0.924	*Cebpg*	0.355	*Traf4*	0.784	*Tmem9*	0.810
Fdxr	0.911	*Kcnf1*	0.337	*Hgs*	0.734	*Nudt9*	0.805
Slc19a1	0.894	*3110043O21Rik*	0.326	*Nt5dc3*	0.726	*Serp1*	0.784
Lonp1	0.869	*Tra2a*	0.310	*Cdk12*	0.680	*Capn5**	0.740
Dusp1	0.847	*Papd5*	0.289	*Trak1*	0.666	*Unc50*	0.720
Ccrn4l	0.821	*Mafg*	0.272	*Usp40*	0.659	*Fem1a*	0.688
A930007I19Rik	0.813	*Sh3bp1*	0.271	*Hspa1l*	0.610	*Oaf*	0.653
Thbs1	0.808	*Scamp3*	0.241	*Sfmbt2*	0.587	*Fstl1*	0.639
Bcl2l1	0.802	*Epha2*	0.223	*Ier2*	0.558	*Krt14**	0.637
Bend4	0.801	*Plekhm1*	0.220	*Lin37*	0.549	*Mrgprf**	0.613
Doc2a	0.795	*Lhfpl2*	0.126	*Cass4*	0.522	*B3gnt9*	0.604
Pfas	0.778	*Lad1*	0.077	*Slc29a2*	0.521	*Psmf1*	0.602
Gm11508	0.758			*Slc5a3*	0.501	*Kdelr3*	0.580
Jmjd6	0.756	**Acute_Darkturquoise**		*Arrdc4*	0.501	*Selk*	0.563
Plk2	0.722	**Gene**	**K_{IM}**	*Phf8*	0.471	*Msln**	0.556
Rassf1	0.710	*Fut4*	1.000	*Pim3*	0.442	*Asf1a*	0.555
Gm13199	0.705	*Rp2h*	0.963	*Gm15228*	0.434	*Pla2g4c*	0.507
Rbm14	0.696	*Itm2c*	0.923	*Cpeb4*	0.430	*Ahrr*	0.504
Ampd2	0.680	*Vcam1*	0.893	*Urb1*	0.398	*Col18a1**	0.493
Mrps10	0.671	*Gm26924*	0.870	*Irak3*	0.398	*Gm16174*	0.485
Htr1b	0.668	*Gm12913*	0.865	*Usp3*	0.387	*Upk1b*	0.439
Mettl13	0.656	*Nxt2*	0.842	*Tlr6*	0.384	*Atp9a*	0.435
Oxnad1	0.653	*Gm15564*	0.695	*Zfp655*	0.366	*Gm12475*	0.396
Mogs	0.637	*Prcp*	0.668	*Crlf2*	0.338	*Lax1*	0.355
Gm16229	0.617	*Ccl5*	0.654	*Smox*	0.329	*Zfp449*	0.340
Lrdd	0.606	*Rit1*	0.649	*Plekhm2*	0.228	*Mgat1**	0.275
Smpd4	0.602	*Tpgs1*	0.626	*Gm16175*	0.112	*Cd248**	0.261
Tcirg1	0.600	*B3galnt1*	0.588			*Prune2*	0.201
1700030J22Rik	0.599	*Igkv1-122*	0.481	**Acute_Darkgreen**		*Mocs1*	0.193
Neu1	0.598	*Rab18*	0.471	**Gene**	**K_{IM}**	*Plbd2*	0.193
Cstf2	0.598	*Pld3*	0.454	*Mfap3*	1	*Tusc1*	0.143
Furin	0.590	*Pparg*	0.357	*4930524O07Rik*	0.996	*Dnajb1**	0.101
Slc7a6	0.585	*Gm8902*	0.330	*Gm16001*	0.976		
Selp	0.585	*Sept10*	0.244	*Arsg*	0.911	**Chronic_Darkturquoise**	
Gm12201	0.571			*Miat*	0.875	**Gene**	**K_{IM}**
Mrpl37	0.564	**Acute_Darkgrey**		*Gm24187*	0.875	*Gpr176*	1
Pusl1	0.561	**Gene**	**K_{IM}**	*Gm23935*	0.873	*Xcl1*	0.966
2410004B18Rik	0.553	*Gm9200*	1.000	*Gm24245*	0.873	*Metazoa_SRP*	0.960
Nab2	0.527	*2010204K13Rik*	0.998	*Gm24270*	0.867	*Metazoa_SRP*	0.956
Armc6	0.508	*Rplp1-ps1*	0.989	*Hoxa5*	0.805	*Kirrel*	0.932
Kbtbd8	0.494	*Gm26377*	0.944	*Zzef1*	0.773	*BC048507*	0.875
Ddx11	0.491	*Psma8*	0.883	*Pld2*	0.760	*Gm24105*	0.802
Gm13904	0.483	*Habp2*	0.834	*Plek2*	0.591	*Rpph1*	0.780
Exoc1	0.479	*Uqcrh*	0.820	*Etohi1*	0.533	*Rai14*	0.643
Csf2ra	0.479	*Gm6206*	0.792	*Hoxa3*	0.498	*Gm22179*	0.618
Zfp948	0.463	*1810043H04Rik*	0.689	*Clec4b2*	0.486	*Taf5l*	0.606
Gm16194	0.462	*Rpp14*	0.627	*Gm13031*	0.481	*Enah*	0.395

Acute_Magenta (cont)	
Gene	**K_{IM}**
Tbrg4	0.452
Phlda1	0.449
Tsfm	0.443
Rab44	0.427
Adam12	0.424

Acute_Darkgrey (cont)	
Gene	**K_{IM}**
Siglece	0.569
Fis1	0.522
Gm11307	0.491
Emc6	0.353
Lyrm4	0.124

Acute_Darkgreen (cont)	
Gene	**K_{IM}**
Hoga1	0.267
Zfp518b	0.263
Trio	0.177

Chronic_Darkturquoise (cont)	
Gene	**K_{IM}**
Dnase1l3	0.19
1700007L15Rik	0.158
Rpl5-ps1	0.131
Eif3s6-ps1	0.130
Trbv12-2	0.079

Chronic_Darkred	
Gene	**K_{IM}**
Plagl1	1
Slc9b2	0.942
Slamf6	0.905
Cx3cl1	0.897
Lrba	0.856
Idi1	0.831
Slain1	0.699
Sqle	0.640
Tnfsf11	0.623
Gm13502	0.607
Paip2b	0.600
Ap1ar	0.578
Drc1	0.559
Cyp51	0.553
Lss	0.525
Trbv12-1	0.491
Etv5	0.465
Ccdc141	0.451
Snap47	0.324
Igfbp2	0.321
Angptl7	0.311
Smco4	0.296
Fam26e	0.184
Fgf7	0.124
Adcy1	0.104

Chronic_Darkgreen	
Gene	**K_{IM}**
Esr1	1
Gstm4	0.999
Fam188b	0.949
Lrrn1	0.922
Rit1	0.807
Galnt18	0.657
AB124611	0.635
Dcxr	0.622
Pafah1b1-ps1	0.621
Mgst1	0.545
Tmem50a	0.535
Bin3	0.493
H2-T3	0.442
Ppp1r2	0.387
Hpcal1	0.352
Pnpla2	0.317
1700009P17Rik	0.242
H2afv	0.237
Vkorc1	0.083
Esr1	1

The results of this thesis have been submitted as a journal article that is under revision:

Systems analysis reveals complex biological processes in virus infection fate decisions

Jordi Argilaguet[1,12], Mireia Pedragosa[1,12], Anna Esteve-Codina[2,3,12], Graciela Riera[1], Enric Vidal[4], Cristina Peligero-Cruz[1,5], David Andreu[7], Tsuneyasu Kaisho[8,9], Gennady Bocharov[10], Burkhart Ludewig[6], Simon Heath[2,3] and Andreas Meyerhans[1,11,13,*]
*Correspondence: andreas.meyerhans@upf.edu

Affiliations/Institutions:
[1]Infection Biology Laboratory, Department of Experimental and Health Sciences, Universitat Pompeu Fabra, Barcelona, Spain.
[2]Center for Genomic Regulation (CRG), Barcelona Institute of Science and Technology, Barcelona, Spain.
[3]Universitat Pompeu Fabra (UPF), Barcelona, Spain
[4]Centre de Recerca en Sanitat Animal (CReSA-IRTA-UAB), Universitat Autònoma de Barcelona, Barcelona, Spain.
[5]Present address: Department of Immunology, Weizmann Institute of Science, Rehovot, Israel.
[6]Institute for Immunobiology, Kantonsspital St. Gallen, St. Gallen, Switzerland.
[7]Laboratory of Proteomics and Protein Chemistry, Universitat Pompeu Fabra, Barcelona, Spain.
[8]Department of Immunology, Institute of Advanced Medicine, Wakayama Medical University, Wakayama, Japan.
[9]Laboratory for Immune Regulation, World Premier International Research Center Initiative, Immunology Frontier Research Center, Osaka University, Osaka, Japan.
[10]Institute of Numerical Mathematics, Russian Academy of Sciences, Moscow, Russia.
[11]Institució Catalana de Recerca i Estudis Avançats, Barcelona, Spain.
[12]These authors contributed equally.

Argilaguet J, Pedragosa M, Esteve-Codina A, Riera G, Vidal E, Peligero-Cruz C, et al. Systems analysis reveals complex biological processes during virus infection fate decisions. Genome Res. 2019 Jun;29(6):907–19. DOI: 10.1101/gr.241372.118

DISCUSSION

In this thesis we analyzed, on a systems level, infection-fate-specific gene signatures and the resulting adaptive processes of the host to an overwhelming virological threat. We used the well-established lymphocytic choriomeningitis virus infection mouse model, which has been instrumental to detect many fundamental processes in the virus-immune system crosstalk that are also relevant in human virus infections. We show, first, spleen-derived transcriptomes reflect different virus infection stages. Second, clustering of the time-resolved transcriptomes into coexpression modules reveal several infection fate-specific networks. Third, in chronic infection, there is an early attenuation of macrophage-mediated inflammation that occurs prior to the onset of T cell exhaustion. And finally, in the time window when $CD8^+$ T cell exhaustion appears, there is a recruitment of cross-presenting dendritic cells that contributes to the maintenance of an antiviral cytotoxic T cell response and participates in viral control in the chronic infection phase. Together our data demonstrate a delicate adaptation process towards an overwhelming virus infection with both immunosuppressive and immunostimulatory processes. Furthermore, it fills a knowledge gap regarding the mechanisms of effector T cell maintenance and provides a new immune cell subset for targeted therapeutic vaccination.

1. Systems analysis of virus infection fate

Non-lethal pathogenic viral infections are either acutely resolved or become chronic. While this fate decision is made during the primary infection phase, it is incompletely understood and a systems view is lacking. In this thesis, we characterized spleen transcriptome changes during the course of acute and chronic viral infections. Interestingly, both infection fates are readily distinguished by their sequential splenic transcriptomes. Hierarchical clustering across all samples revealed several groups corresponding to different infection stages: naive mice and mice in memory phase, early and late effector responses, and chronic infection phase. Thus, distinct virus infection phases exhibit separated transcriptome signatures in the lymphoid tissue. However, although we were able to see this global picture of the differentially expressed genes after acute and chronic infections, this conventional analysis did not show differentiating molecular signatures, neither in the number of genes involved nor in the biological pathways enriched, thus highlighting the need of more complex bioinformatic analysis to decipher the molecular signatures linked to the corresponding phenotypes. To overcome this need, we used gene coexpression network analysis of spleen transcriptomes and decomposed the complex host response against the invading virus into several modules of highly coexpressed genes. From the whole transcriptome, that covers nearly 14000 differentially expressed

genes, 23 modules were obtained for each infection group. The expression patterns of these modules already depict the complexity of the coordinated host response against infection, and can be linked to molecular events with biological meaning. Module preservation analysis then permitted to better understand the differentiating and the common traits between both infections. We found that a large number of genes participate in biological pathways that are common in acute and chronic infections, and only few are specific for each infection outcome. From the analysis of those modules that are specific of chronic infection, we could find differentiating traits at day 9 postinfection when exhaustion appears. However, close inspection of the coexpression modules demonstrated acute-infection-specific molecular events at day 6 before T cell exhaustion becomes apparent. Thus, suggesting that the decision point to downregulate immune responses towards an overwhelming virus threat is already taken before T cells shut off their effector functions. Whether this decision point lies even earlier remains to be determined. So far, early innate immune responses represented i.e. by modules containing type I IFN genes are very similar in acute and chronic infections, and differences come up only from day 6 onwards.

In addition to these global characteristics, we were also able to link specific genes and pathways to critical, already established phenotypes associated with both infection fates including the effective LCMV-specific T cell response as well as T cell exhaustion and hypergammaglobulinemia, a condition characterized by non-specific immunoglobulins as a result of switching from IgM to IgG (Hunziker et al. 2003). This validates our approach for analyzing virus infection fates and leaves a rich comprehensive data set for further, more specific analyses.

2. Early attenuation of inflammatory response in chronic infection

Infection-fate-specific module information provide a firm basis to reveal specific, physiologically relevant changes in the infected host organism. An intriguing observation was that the infection-fate-specific modules contained rather few genes that when tested for their expression dynamics in the respective other infection fate, these genes appeared not corregulated and linked within different modules. As modules are linked to biological pathways, it would seem that rather few of such pathways are responsible for infection fate discrimination. This notion may not only help to define diagnostic biomarker for predicting infection outcomes but also hint to regulators of pathways that may direct phenotype evolution over time. Indeed, the acute-grey60 module with its 31 genes that have an expression peak at day 6, is a good

example. Starting from a GO enrichment analysis of its genes we subsequently identified important differences in early monocytic cell polarization with an M1-type profile in acute infection and cells with an attenuated phenotype during chronic infection. Previous studies have described a skewing of monocytic cells towards MDSCs in chronic LCMV infections of mice (Norris et al. 2013) and in HIV, HBV and HCV infections in humans (Qin et al. 2013; Cai et al. 2013; Pallett et al. 2015). MDSCs appear during the primary infection phase and have been characterized, i.e. by transcriptome analysis at day 14 post-chronic LCMV clone 13 infection, a few days after T cell exhaustion becomes apparent (Norris et al. 2013). Our own RNA-seq results from isolated monocytic cells at day 6 postinfection now point to an even earlier phenotypic shift. While splenic cells from acute infection show a typical inflammatory signature, the respective cells in chronic infection are already markedly different with a reduction of inflammatory markers and an expression of genes linked to alternative macrophage differentiation and anti-inflammation. Interestingly, this early monocytic cell skewing was associated with histological changes in the spleen. Acutely-infected mice develop spleen fibrosis that is maintained even when the virus is already well controlled, while in chronic infection, fibrosis was almost absent (Figure R5C and R5D). Although the direct evidence for a causal link between the splenic monocyte/macrophage phenotypes and fibrosis development is still missing, the known features of tissue macrophages in tissue injury, fibrosis and repair are well in line with our observations (Wynn & Vannella 2016; Sugimoto et al. 2016).

3. XCL1-XCR1 crosstalk for T cell effector maintenance

Concomitant with $CD8^+$ T cell exhaustion during chronic infection, $XCR1^+$ DC number increase in spleen. This intriguing association was suspected and then experimentally verified after analyzing the fate-specific module chronic-darkturquoise that showed gene upregulation from day 7 to day 9 and included XCL1, a chemokine produced by NK and activated $CD8^+$ T cells and known to specifically attract XCR1-expressing cross-presenting DCs. Subsequent depletion experiments of $XCR1^+$ DCs using high-dose $LCMV_{Doc}$-infected XCR1-DTRvenus animals resulted in a reduction of virus-specific $CD8^+$ T cells and a concurrent increase in viral loads (Figure R7C and R7D) not only in spleen but also in lung and kidney. However, as downregulation of T cell effector function by exhaustion is a mechanism to avoid immunopathology (Cornberg et al. 2013b), as is attenuation of inflammatory macrophages and generation of MDSCs (Medzhitov et al. 2012), why should a host organism at the same time expand a subtype of antigen-presenting cells that are highly potent in priming and boosting novel T cell responses?

This fundamental issue may simply highlight two important aspects within the in vivo virus-immune system cross-talk. First, the immune system has to shut down when confronted with an overwhelming viral threat. A high-dose $LCMV_{Doc}$ infection requires an adaptation of the immune response and viral load dynamics such that it levels below a life-threatening situation. This is achieved by a variety of immunosuppressive mechanisms of which T cell exhaustion and the generation of MDSCs are important components. Second, the immune system does not surrender completely to an overwhelming threat but maintains partial control and restricts virus overloads. One possible way for this seems to be a feedback regulation involving cells from the population of virus-specific $CD8^+$ T cells that become exhausted. Indeed, the population of LCMV-specific $CD8^+$ T cells that becomes exhausted contains cells that produce XCL1 (Figure R6E) and thus can set up $XCR1^+$ DC recruitment and cytotoxic T cell stimulation and effector cell maintenance. Overall, this argues for the operation of virus-threat-sensing host mechanisms that adapt the immune system effectors to minimize damage and the XCL1-XCR1 axis of being part of a functional adaptation to the chronic infection phase to maintain the virus under control.

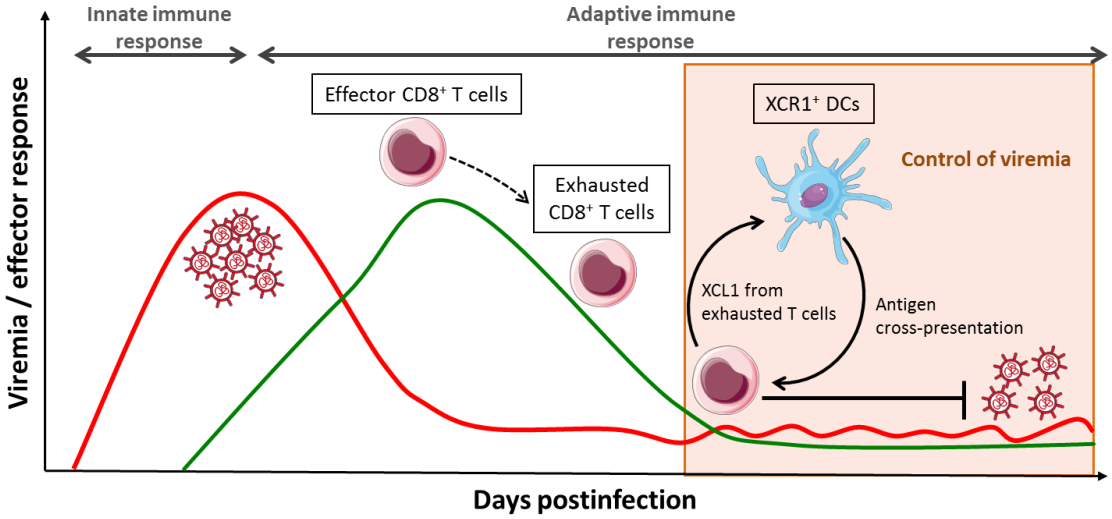

Figure D1. Schematic view of virus loads and CD8 T cells during a chronic infection. Schematic dynamics for virus (red line) and CD8+ effector T cells (green line) are given within an arbitrary time scale. The regulatory loop linking exhaustion of CD8+ T cells with maintenance of a low level effector response involving XCR1+ DCs is highlighted.

4. Using Xcr1 DCs as a target for therapeutic vaccination

The data presented here and previous work from others are concordant with the view of a dichotomy between immunosuppression and immune activation during the adaptation towards an overwhelming virus threat. First, without $CD8^+$ T cell exhaustion, an overwhelming LCMV infection is life threatening (Barber et al. 2006; Moskophidis et al. 1995). Second, $CD8^+$ T cell exhaustion and the generation of MDSCs are common features of chronic LCMV infection of mice as well as chronic human infections with HIV, HBV and HCV (Vollbrecht et al. 2012; Qin et al. 2013; Cai et al. 2013; Norris et al. 2013). Third, blocking of immunosuppressive mechanisms during chronic infections can expand effector functions and decrease virus steady state levels (Schmitz et al. 1999; Jin et al. 1999). Fourth, despite the presence of exhausted T cells in chronic infections, a significant level of cytotoxic T cell activity remains detectable that maintains partial virus control (Allen et al. 2005).

How may these observations be exploited for host benefit? Recent publications have shown that virus-specific $CXCR5^+$ $CD8^+$ T cells are the population that expand most efficiently after immune checkpoint inhibition (Im et al. 2016; He et al. 2016). They are, besides NK cells, the main producer of XCL1 in the chronic infection phase (Figure 6C). XCL1 is elevated in HIV-infected elite controllers (Jacobs et al. 2017) and its receptor XCR1 is solely expressed on cross-presenting DCs (Dorner et al. 2009) that are specifically upregulated during the chronic infection phase (Figure 7A and S5C). Therefore, enforcing the XCL1-XCR1 axis in an immunotherapeutic intervention seems a promising strategy to better control chronic virus infections. One option in this direction would be the already established targeting of immunogens to $XCR1^+$ DCs via linkage to XCL1 itself or to a XCR1-targeting antibody (Fossum et al. 2015). The advantage of using XCL1 over antibodies fused to antigen is that chemokines do not induce immune responses in its original host but induce signaling upon binding to cell surface receptors adding an additional adjuvant effect. Furthermore, the XCR1 receptor has been reported to be expressed in $CD8^+$ residential and interstitial DCs in mice (Dorner et al. 2009), in macaques (Dutertre et al. 2014), and in sheep (Contreras et al. 2010) thus, suggesting a possible easier technology transfer to other species when compared to the use of specific antibodies for each individual species. Combining such immunotherapeutic vaccination with checkpoint inhibition may then allow effector cell expansion enhanced by a positive feedback loop and thus a greater increase in the effector cell to virus ratio.

CONCLUSIONS

The main conclusions from the results presented in this thesis are the following:

Time-resolved systems analysis of spleen transcriptomes reveals the main biological pathways in acute and chronic LCMV infection

- Spleen transcriptomes match with distinct stages of acute and chronic LCMV infection
- Cellular and humoral adaptive responses are disassociated in chronic infection
- Infection fate-specific coexpression networks contain few genes

Early attenuation of inflammatory monocytic cells is linked to fibrosis prevention

- Inflammatory monocytes/macrophages during chronic infection shift to an anti-inflammatory profile before T cell exhaustion appears
- Presence of these cells correlates with fibrosis prevention in chronic infection

XCL1-XCR1 communication is part of a functional adaptation to chronic infection

- Gene coexpression analysis reveals XCL1 as an important chemokine during the establishment of the chronic infection phase
- XCL1 produced by NK and virus-specific $CD8^+$ T cells during chronic infection results in an increase of XCR1+ DCs numbers in spleen
- Depletion of $XCR1^+$ DCs results in reduction of virus-specific $CD8^+$ T cells and an increase in viral loads

Our results with the LCMV infection mouse model suggest directions for immunotherapeutic strategies to better control or even cure persistent infections in humans

ANNEXES

ANNEX1

List of abbreviations

Arg2	Arginase 2
α-DG	Alpha Dystroglycan
BSA	Bovine serum albumin
BTLA	B and T lymphocyte attenuator
CTL	Cytotoxic T cell
DC	Dendritic cell
DTR	Diphtheria toxin receptor
EDTA	Ethylenediaminetetraacetic acid
FACS	Fluorescence activated cell sorting
GO	Gene ontology
GPC	Glycoprotein
HBC	Hepatitis B virus
HCV	Hepatitis C virus
hi	High
HIV	Human immunodeficiency virus
IFN	Interferon
IgG	Immunoglobulin G
IL	Interleukin
IRG	Intergenic region
KLRG1	Killer-cell lectin like receptor G1
Lag3	Lymphocyte activation gene 3
LCMV	Lymphocytic choriomeningitis virus
lo	Low
MDSC	Myeloid derived suppressor cell
MHCII	Major histocompatibility complex II
NK cell	Natural killer cell
NOS2	Nitric oxide synthase 2

PBS	Phosphate-buffered saline
PD1	Programed cell death 1
PDL1	Programed cell death ligand 1
RNA	Ribonucleic acid
RNP	Ribonucleoprotein
RPMI	Roswell Park Memorial Institute Medium
SEM	Standard error of the mean
SIV	Simian immunodeficiency virus
TIGIT	T cell immunoglobulin and ITIM domain
TGFβ	Tumour necrosis factor β
Tim3	T cell immunoglobulin mucin 3
Treg	Regulatory T cell
XCL1	X-C motif chemokine ligand 1
XCR1	X-C motif chemokine receptor 1
WGCNA	Weighted gene coexpression network analysis

REFERENCES

A

Ahmadzadeh, M. et al., 2009. Tumor antigen-specific CD8 T cells infiltrating the tumor express high levels of PD-1 and are functionally impaired. *Blood,* 114(8), pp.1537–1544.

Allen, T.M. et al., 2005. Selective escape from CD8+ T-cell responses represents a major driving force of human immunodeficiency virus type 1 (HIV-1) sequence diversity and reveals constraints on HIV-1 evolution. *Journal of virology*, 79(21), pp.13239–13249.

Asabe, S. et al., 2009. The size of the viral inoculum contributes to the outcome of hepatitis B virus infection. *Journal of virology*, 83(19), pp.9652–9662.

B

Bachmann, M.F. et al., 2007. Differential role of IL-2R signaling for CD8 T cell responses in acute and chronic viral infections. *European journal of immunology*, 37(6), pp.1502–1512.

Barber, D.L. et al., 2006. Restoring function in exhausted CD8 T cells during chronic viral infection. *Nature*, 439(7077), pp.682–687.

Barnaba, V. & Schinzari, V., 2013. Induction, control, and plasticity of Treg cells: the immune regulatory network revised? *European journal of immunology*, 43(2), pp.318–322.

Barr, T., Carlring, J. & Heath, A., 2006. Co-stimulatory agonists as immunological adjuvants. *Vaccine*, 24(17), pp.3399–3407.

Battegay, M. et al., 1994. Enhanced establishment of a virus carrier state in adult CD4+ T-cell-deficient mice. *Journal of virology*, 68(7), pp.4700–4704.

Battegay, M. et al., 1991. Quantification of lymphocytic choriomeningitis virus with an immunological focus assay in 24- or 96-well plates. *Journal of virological methods*, 33(1-2), pp.191–198.

Belkaid, Y. & Tarbell, K., 2009. Regulatory T cells in the control of host-microorganism interactions (*). A*nnual review of immunology, 27, pp.551–589.*

Benoist, C. & Mathis, D., 2012. Treg cells, life history, and diversity. *Cold Spring Harbor perspectives in biology, 4(9), p.a007021.*

Bergthaler, A. et al., 2010. Viral replicative capacity is the primary determinant of lymphocytic choriomeningitis virus persistence and immunosuppression. *Proceedings of the National Academy of Sciences of the United States of America*, 107(50), pp.21641–21646.

Bertoletti, A. & Ferrari, C., 2012. Innate and adaptive immune responses in chronic hepatitis B virus infections: towards restoration of immune control of viral

infection. *Gut*, 61(12), pp.1754–1764.

Betts, M.R. et al., 2006. HIV nonprogressors preferentially maintain highly functional HIV-specific CD8+ T cells. *Blood, 107(12), pp.4781–4789.*

Blackburn, S.D. et al., 2009. Coregulation of CD8+ T cell exhaustion by multiple inhibitory receptors during chronic viral infection. *Nature immunology*, 10(1), pp.29–37.

Blackburn, S.D. et al., 2008. Selective expansion of a subset of exhausted CD8 T cells by αPD-L1 blockade. *Proceedings of the National Academy of Sciences*, 105(39), pp.15016–15021.

Bocharov, G. et al., 2004. Underwhelming the immune response: effect of slow virus growth on CD8+-T-lymphocyte responses. *Journal of virology*, 78(5), pp.2247–2254.

Boehm, T., 2016. Form follows function, function follows form: how lymphoid tissues enable and constrain immune reactions. *Immunological reviews*, 271(1), pp.4–9.

Brooks, D.G., Trifilo, M.J., et al., 2006. Interleukin-10 determines viral clearance or persistence in vivo. *Nature medicine*, 12(11), pp.1301–1309.

Brooks, D.G., McGavern, D.B. & Oldstone, M.B.A., 2006. Reprogramming of antiviral T cells prevents inactivation and restores T cell activity during persistent viral infection. *The Journal of clinical investigation*, 116(6), pp.1675–1685.

Brooks, D.G. et al., 2008. IL-10 and PD-L1 operate through distinct pathways to suppress T-cell activity during persistent viral infection. *Proceedings of the National Academy of Sciences of the United States of America, 105(51), pp.20428–20433.*

Buchmeier, M.J. et al., 1980. The Virology and Immunobiology of Lymphocytic Choriomeningitis Virus Infection. In *Advances in Immunology*. pp. 275–331.

Burrack, K.S. & Morrison, T.E., 2014. The role of myeloid cell activation and arginine metabolism in the pathogenesis of virus-induced diseases. *Frontiers in immunology*, 5, p.428.

Byrne, J.A., Ahmed, R. & Oldstone, M.B., 1984. Biology of cloned cytotoxic T lymphocytes specific for lymphocytic choriomeningitis virus. I. Generation and recognition of virus strains and H-2b mutants. *Journal of immunology* , 133(1), pp.433–439.

C

Cai, G. & Freeman, G.J., 2009. The CD160, BTLA, LIGHT/HVEM pathway: a bidirectional switch regulating T-cell activation. *Immunological reviews, 229(1), pp.244–258.*

Cai, W. et al., 2013. Clinical significance and functional studies of myeloid-derived suppressor cells in chronic hepatitis C patients. *Journal of clinical immunology*, 33(4), pp.798–808.

Cameron, M.J. & Kelvin, D.J., 2003. Cytokines and chemokines--their receptors and their genes: an overview. *Advances in experimental medicine and biology*, 520, pp.8–32.

Cao, W., 1998. Identification of -Dystroglycan as a Receptor for Lymphocytic Choriomeningitis Virus and Lassa Fever Virus. *Science*, 282(5396), pp.2079–2081.

Cheng, L. et al., 2017. Blocking type I interferon signaling enhances T cell recovery and reduces HIV-1 reservoirs. *The Journal of clinical investigation*, 127(1), pp.269–279.

Cheng, Y., Ping, J. & Chen, J., 2017. Identification of Potential Gene Network Associated with HCV-Related Hepatocellular Carcinoma Using Microarray Analysis. *Pathology oncology research: POR*. Available at: http://dx.doi.org/10.1007/s12253-017-0273-8.

Clerici, M. et al., 1994. Role of interleukin-10 in T helper cell dysfunction in asymptomatic individuals infected with the human immunodeficiency virus. *The Journal of clinical investigation*, 93(2), pp.768–775.

Cole, G.A., Nathanson, N. & Prendergast, R.A., 1972. Requirement for Θ-Bearing Cells in Lymphocytic Choriomeningitis Virus-induced Central Nervous System Disease. *Nature*, 238(5363), pp.335–337.

Cornberg, M. et al., 2013a. Clonal Exhaustion as a Mechanism to Protect Against Severe Immunopathology and Death from an Overwhelming CD8 T Cell Response. *Frontiers in immunology*, 4. Available at: http://dx.doi.org/10.3389/fimmu.2013.00475.

Cornberg, M. et al., 2013b. Clonal exhaustion as a mechanism to protect against severe immunopathology and death from an overwhelming CD8 T cell response. *Frontiers in immunology*, 4, p.475.

Crawford, A. et al., 2014. Molecular and transcriptional basis of $CD4^+$ T cell dysfunction during chronic infection. *Immunity*, 40(2), pp.289–302.

Crawford, A. & Wherry, E.J., 2009. The diversity of costimulatory and inhibitory receptor pathways and the regulation of antiviral T cell responses. *Current opinion in immunology*, 21(2), pp.179–186.

D

Day, C.L. et al., 2006. PD-1 expression on HIV-specific T cells is associated with T-cell exhaustion and disease progression. *Nature*, 443(7109), pp.350–354.

Dietze, K.K. et al., 2011. Transient depletion of regulatory T cells in transgenic mice reactivates virus-specific CD8+ T cells and reduces chronic retroviral set points. *Proceedings of the National Academy of Sciences of the United States of America*, 108(6), pp.2420–2425.

Dittmer, U. et al., 2004. Functional impairment of CD8(+) T cells by regulatory T cells during persistent retroviral infection. *Immunity*, 20(3), pp.293–303.

Doering, T.A. et al., 2012. Network analysis reveals centrally connected genes and pathways involved in CD8+ T cell exhaustion versus memory. *Immunity*, 37(6), pp.1130–1144.

Dorner, B.G. et al., 2009. Selective expression of the chemokine receptor XCR1 on cross-presenting dendritic cells determines cooperation with CD8+ T cells. *Immunity*, 31(5), pp.823–833.

Draenert, R. et al., 2004. Immune selection for altered antigen processing leads to cytotoxic T lymphocyte escape in chronic HIV-1 infection. *The Journal of experimental medicine*, 199(7), pp.905–915.

Dyavar Shetty, R. et al., 2012. PD-1 blockade during chronic SIV infection reduces hyperimmune activation and microbial translocation in rhesus macaques. *The Journal of clinical investigation*, 122(5), pp.1712–1716.

E

Ehl, S. et al., 1998. The impact of variation in the number of CD8(+) T-cell precursors on the outcome of virus infection. *Cellular immunology*, 189(1), pp.67–73.

Evans, R. & Alexander, P., 1972. Mechanism of immunologically specific killing of tumour cells by macrophages. *Nature, 236(5343), pp.168–170.*

F

Fahey, L.M. & Brooks, D.G., 2010. Opposing positive and negative regulation of T cell activity during viral persistence. *Current opinion in immunology, 22(3), pp.348–354.*

Farmer, T.W. & Janeway, C.A., 1942. INFECTIONS WITH THE VIRUS OF LYMPHOCYTIC CHORIOMENINGITIS. *Medicine*, 21(1), pp.65–94.

Feinberg, M.B. & Ahmed, R., 2012. Born this way? Understanding the immunological basis of effective HIV control. *Nature immunology*, 13(7), pp.632–634.

Fitzgerald-Bocarsly, P. & Jacobs, E.S., 2010. Plasmacytoid dendritic cells in HIV infection: striking a delicate balance. *Journal of leukocyte biology*, 87(4), pp.609–620.

Fontenot, J.D., Gavin, M.A. & Rudensky, A.Y., 2003. Foxp3 programs the development and function of CD4+CD25+ regulatory T cells. *Nature immunology, 4(4), pp.330–336.*

Fossum, E. et al., 2015. Vaccine molecules targeting Xcr1 on cross-presenting DCs induce protective CD8+ T-cell responses against influenza virus. *European journal of immunology*, 45(2), pp.624–635.

Fröhlich, A. et al., 2009. IL-21R on T cells is critical for sustained functionality and control of chronic viral infection. *Science*, 324(5934), pp.1576–1580.

Fukuyama, S. & Kawaoka, Y., 2011. The pathogenesis of influenza virus infections: the contributions of virus and host factors. *Current opinion in immunology*, 23(4), pp.481–486.

G

Gallaher, W.R., DiSimone, C. & Buchmeier, M.J., 2001. The viral transmembrane superfamily: possible divergence of Arenavirus and Filovirus glycoproteins from a common RNA virus ancestor. *BMC microbiology*, 1, p.1.

Guo, X. et al., 2017. Identification of breast cancer mechanism based on weighted gene coexpression network analysis. *Cancer gene therapy*, 24(8), pp.333–341.

Gallimore, A. et al., 1998. Induction and exhaustion of lymphocytic choriomeningitis virus-specific cytotoxic T lymphocytes visualized using soluble tetrameric major histocompatibility complex class I-peptide complexes. *The Journal of experimental medicine, 187(9), pp.1383–1393.*

Greenwald, R.J., Freeman, G.J. & Sharpe, A.H., 2005. The B7 family revisited. *Annual review of immunology,* 23, pp.515–548.

Guardo, A.C. et al., 2017. Preclinical evaluation of an mRNA HIV vaccine combining rationally selected antigenic sequences and adjuvant signals (HTI-TriMix). *AIDS , 31(3),* pp.321–332.

H

Hangartner, L., Zinkernagel, R.M. & Hengartner, H., 2006. Antiviral antibody responses: the two extremes of a wide spectrum. *Nature reviews. Immunology*, 6(3), pp.231–243.

Ha, S.-J. et al., 2008. Enhancing therapeutic vaccination by blocking PD-1–mediated inhibitory signals during chronic infection. *The Journal of experimental medicine*, 205(3), pp.543–555.

He, R. et al., 2016. Follicular CXCR5- expressing CD8(+) T cells curtail chronic viral infection. *Nature*, 537(7620), pp.412–428.

Hiroishi, K. et al., 1997. Cytotoxic T lymphocyte response and viral load in hepatitis C virus infection. *Hepatology* , 25(3), pp.705–712.

Hori, S., 2003. Control of Regulatory T Cell Development by the Transcription Factor Foxp3. *Science, 299(5609), pp.1057–1061.*

Horvath, S. et al., 2006. Analysis of oncogenic signaling networks in glioblastoma identifies ASPM as a molecular target. *Proceedings of the National Academy of Sciences of the United States of America, 103(46), pp.17402–17407.*

Huang, D.W., Sherman, B.T. & Lempicki, R.A., 2009. Systematic and integrative analysis

of large gene lists using DAVID bioinformatics resources. *Nature protocols*, 4(1), pp.44–57.

Hunziker, L. et al., 2003. Hypergammaglobulinemia and autoantibody induction mechanisms in viral infections. *Nature immunology*, 4(4), pp.343–349.

I

Im, S.J. et al., 2016. Defining CD8+ T cells that provide the proliferative burst after PD-1 therapy. *Nature*, 537(7620), pp.417–421.

J

Jacobs, E.S. et al., 2017. Cytokines Elevated in HIV Elite Controllers Reduce HIV Replication In Vitro and Modulate HIV Restriction Factor Expression. *Journal of virology*, 91(6). Available at: http://dx.doi.org/10.1128/JVI.02051-16.

Jeong, H. et al., 2001. Lethality and centrality in protein networks. *Nature*, 411(6833), pp.41–42.

Jin, H.-T. et al., 2010. Cooperation of Tim-3 and PD-1 in CD8 T-cell exhaustion during chronic viral infection. *Proceedings of the National Academy of Sciences of the United States of America*, 107(33), pp.14733–14738.

Jin, H.-T. et al., 2011. Mechanism of T cell exhaustion in a chronic environment. *BMB reports*, 44(4), pp.217–231.

Jin, X. et al., 1999. Dramatic rise in plasma viremia after CD8(+) T cell depletion in simian immunodeficiency virus-infected macaques. *The Journal of experimental medicine*, 189(6), pp.991–998.

K

Kahan, S.M., Wherry, E.J. & Zajac, A.J., 2015. T cell exhaustion during persistent viral infections. *Virology*, 479-480, pp.180–193.

Khattri, R. et al., 2003. An essential role for Scurfin in CD4+CD25+ T regulatory cells. *Nature immunology, 4(4), pp.337–342.*

Kim, J.V. et al., 2009. Myelomonocytic cell recruitment causes fatal CNS vascular injury during acute viral meningitis. *Nature*, 457(7226), pp.191–195.

Klenerman, P. & Hill, A., 2005. T cells and viral persistence: lessons from diverse infections. *Nature immunology*, 6(9), pp.873–879.

Kroczek, R.A. & Henn, V., 2012. The Role of XCR1 and its Ligand XCL1 in Antigen Cross-Presentation by Murine and Human Dendritic Cells. *Frontiers in immunology*, 3, p.14.

Kunz, S. et al., 2003. Mechanisms for lymphocytic choriomeningitis virus glycoprotein cleavage, transport, and incorporation into virions. *Virology*, 314(1), pp.168–178.

Kunz, S., Borrow, P. & Oldstone, M.B.A., 2002. Receptor structure, binding, and cell entry of arenaviruses. *Current topics in microbiology and immunology*, 262, pp.111–137.

L

Landay, A.L. et al., 1996. In vitro restoration of T cell immune function in human immunodeficiency virus-positive persons: effects of interleukin (IL)-12 and anti-IL-10. *The Journal of infectious diseases*, 173(5), pp.1085–1091.

Langfelder, P. & Horvath, S., 2008. WGCNA: an R package for weighted correlation network analysis. *BMC bioinformatics*, 9, p.559.

Lanier, L.L., 1998. NK CELL RECEPTORS. *Annual review of immunology, 16(1), pp.359–393.*

Latchman, Y. et al., 2001. PD-L2 is a second ligand for PD-1 and inhibits T cell activation. *Nature immunology*, 2(3), pp.261–268.

Lechner, F. et al., 2000. Analysis of successful immune responses in persons infected with hepatitis C virus. *The Journal of experimental medicine, 191(9), pp.1499–1512.*

Leong, Y.A. et al., 2016. CXCR5+ follicular cytotoxic T cells control viral infection in B cell follicles. *nature.com*. Available at: https://www.nature.com/ni/journal/v17/n10/abs/ni.3543.html.

Lichterfeld, M. et al., 2004. Loss of HIV-1–specific CD8 T Cell Proliferation after Acute HIV-1 Infection and Restoration by Vaccine-induced HIV-1–specific CD4 T Cells. *The Journal of experimental medicine*, 200(6), pp.701–712.

Lichterfeld, M. et al., 2007. Selective Depletion of High-Avidity Human Immunodeficiency Virus Type 1 (HIV-1)-Specific CD8 T Cells after Early HIV-1 Infection. *Journal of virology*, 81(8), pp.4199–4214.

Li, Q. et al., 2009. Visualizing antigen-specific and infected cells in situ predicts outcomes in early viral infection. *Science*, 323(5922), pp.1726–1729.

M

Macal, M. et al., 2012. Plasmacytoid dendritic cells are productively infected and activated through TLR-7 early after arenavirus infection. *Cell host & microbe*, 11(6), pp.617–630.

Martínez-Sobrido, L. et al., 2007. Differential inhibition of type I interferon induction by arenavirus nucleoproteins. *Journal of virology*, 81(22), pp.12696–12703.

Martínez-Sobrido, L. et al., 2009. Identification of amino acid residues critical for the anti-interferon activity of the nucleoprotein of the prototypic arenavirus lymphocytic choriomeningitis virus. *Journal of virology*, 83(21), pp.11330–11340.

Masson, D. & Tschopp, J., 1985. Isolation of a lytic, pore-forming protein (perforin) from cytolytic T-lymphocytes. *The Journal of biological chemistry*, 260(16), pp.9069–9072.

Matloubian, M., Concepcion, R.J. & Ahmed, R., 1994. CD4+ T cells are required to sustain CD8+ cytotoxic T-cell responses during chronic viral infection. *Journal of virology*, 68(12), pp.8056–8063.

McMichael, A.J. et al., 2010. The immune response during acute HIV-1 infection: clues for vaccine development. *Nature reviews. Immunology*, 10(1), pp.11–23.

Medzhitov, R., Schneider, D.S. & Soares, M.P., 2012. Disease tolerance as a defense strategy. *Science*, 335(6071), pp.936–941.

Miki, Y. et al., 2013. Lymphoid tissue phospholipase A2 group IID resolves contact hypersensitivity by driving antiinflammatory lipid mediators. *The Journal of experimental medicine*, 210(6), pp.1217–1234.

Morrissey, P.J., 1993. CD4 T cells that express high levels of CD45RB induce wasting disease when transferred into congenic severe combined immunodeficient mice. Disease development is prevented by cotransfer of purified CD4 T cells. The *Journal of experimental medicine, 178(1), pp.237–244.*

Moskophidis, D. et al., 1995. Role of virus and host variables in virus persistence or immunopathological disease caused by a non-cytolytic virus. *The Journal of general virology*, 76 (Pt 2), pp.381–391.

Moskophidis, D. et al., 1993. Virus persistence in acutely infected immunocompetent mice by exhaustion of antiviral cytotoxic effector T cells. *Nature*, 362(6422), pp.758–761.

Murali-Krishna, K. et al., 1998. Counting antigen-specific CD8 T cells: a reevaluation of bystander activation during viral infection. *Immunity*, 8(2), pp.177–187.

N

Nakamoto, N. et al., 2008. Functional restoration of HCV-specific CD8 T cells by PD-1 blockade is defined by PD-1 expression and compartmentalization. *Gastroenterology, 134(7), pp.1927–37, 1937.e1–2.*

Nakamoto, N. et al., 2009. Synergistic reversal of intrahepatic HCV-specific CD8 T cell exhaustion by combined PD-1/CTLA-4 blockade. *PLoS pathogens*, 5(2), p.e1000313.

Ng, C.T. et al., 2013. Networking at the level of host immunity: immune cell interactions during persistent viral infections. *Cell host & microbe*, 13(6), pp.652–664.

Nguyen, L.T. & Ohashi, P.S., 2014. Clinical blockade of PD1 and LAG3 — potential mechanisms of action. *Nature reviews. Immunology*, 15(1), pp.45–56.

Norris, B.A. et al., 2013. Chronic but not acute virus infection induces sustained expansion of myeloid suppressor cell numbers that inhibit viral-specific T cell immunity. *Immunity*, 38(2), pp.309–321.

O

Ochsenbein, A.F. et al., 1999. Control of early viral and bacterial distribution and disease by natural antibodies. *Science, 286(5447), pp.2156–2159.*

Okoye, I.S. et al., 2017. Coinhibitory Receptor Expression and Immune Checkpoint Blockade: Maintaining a Balance in CD8+ T Cell Responses to Chronic Viral Infections and Cancer. *Frontiers in immunology*, 8, p.1215.

Oldstone, M.B.A., 2013. Lessons learned and concepts formed from study of the pathogenesis of the two negative-strand viruses lymphocytic choriomeningitis and influenza. *Proceedings of the National Academy of Sciences of the United States of America*, 110(11), pp.4180–4183.

Oldstone, M.B.A., 2006. Viral persistence: Parameters, mechanisms and future predictions. *Virology*, 344(1), pp.111–118.

Oldstone, M.B.A. & Campbell, K.P., 2011. Decoding arenavirus pathogenesis: essential roles for alpha-dystroglycan-virus interactions and the immune response. *Virology*, 411(2), pp.170–179.

Oleinika, K. et al., 2013. Suppression, subversion and escape: the role of regulatory T cells in cancer progression. *Clinical and experimental immunology, 171(1), pp.36–45.*

P

Pallett, L.J. et al., 2015. Metabolic regulation of hepatitis B immunopathology by myeloid-derived suppressor cells. *Nature medicine*, 21(6), pp.591–600.

Pauken, K.E. & Wherry, E.J., 2015. Overcoming T cell exhaustion in infection and cancer. *Trends in immunology*, 36(4), pp.265–276.

Penaloza-MacMaster, P. et al., 2014. Interplay between regulatory T cells and PD-1 in modulating T cell exhaustion and viral control during chronic LCMV infection. *The Journal of experimental medicine*, 211(9), pp.1905–1918.

Perez, M. & de la Torre, J.C., 2003. Characterization of the genomic promoter of the prototypic arenavirus lymphocytic choriomeningitis virus. *Journal of virology*, 77(2), pp.1184–1194.

Petrovas, C. et al., 2006. PD-1 is a regulator of virus-specific CD8 T cell survival in HIV infection. *The Journal of experimental medicine*, 203(10), pp.2281–2292.

Pipkin, M.E. et al., 2010. Interleukin-2 and inflammation induce distinct transcriptional programs that promote the differentiation of effector cytolytic T cells. *Immunity*, 32(1), pp.79–90.

Powrie, F. & Mason, D., 1990. OX-22high CD4+ T cells induce wasting disease with multiple organ pathology: prevention by the OX-22low subset. *The Journal of experimental medicine, 172(6), pp.1701–1708.*

Q

Qin, A. et al., 2013. Expansion of monocytic myeloid-derived suppressor cells dampens T cell function in HIV-1-seropositive individuals. *Journal of virology*, 87(3), pp.1477–1490.

R

Radziewicz, H., Dunham, R.M. & Grakoui, A., 2009. PD-1 tempers Tregs in chronic HCV infection. *The Journal of clinical investigation*, 119(3), pp.450–453.

Rehermann, B. & Nascimbeni, M., 2005. Immunology of hepatitis B virus and hepatitis C virus infection. *Nature reviews. Immunology*, 5(3), pp.215–229.

Richter, K., Perriard, G. & Oxenius, A., 2013. Reversal of chronic to resolved infection by IL-10 blockade is LCMV strain dependent. *European journal of immunology*, 43(3), pp.649–654.

Riviere, Y. et al., 1977. Inhibition by anti-interferon serum of lymphocytic choriomeningitis virus disease in suckling mice. *Proceedings of the National Academy of Sciences*, 74(5), pp.2135–2139.

Robinson, M.D. & Oshlack, A., 2010. A scaling normalization method for differential expression analysis of RNA-seq data. *Genome biology*, 11(3), p.R25.

Rouse, B.T. & Sehrawat, S., 2010. Immunity and immunopathology to viruses: what decides the outcome? *Nature reviews. Immunology, 10(7), pp.514–526.*

S

Sakaguchi, S. et al., 2011. Pillars article: immunologic self-tolerance maintained by activated T cells expressing IL-2 receptor α-chains (CD25). Breakdown of a single mechanism of self-tolerance causes various autoimmune diseases. *J. Immunol. 1995. Journal of immunology , 186(7), pp.3808–3821.*

Sakaguchi, S., 1982. Study on cellular events in post-thymectomy autoimmune oophoritis in mice. II. Requirement of Lyt-1 cells in normal female mice for the prevention of oophoritis. *The Journal of experimental medicine, 156(6), pp.1577–1586.*

Said, E.A. et al., 2010. Programmed death-1–induced interleukin-10 production by

monocytes impairs CD4 T cell activation during HIV infection. *Nature medicine*, 16(4), pp.452–459.

Schacker, T.W. et al., 2006. Lymphatic tissue fibrosis is associated with reduced numbers of naive CD4+ T cells in human immunodeficiency virus type 1 infection. *Clinical and vaccine immunology: CVI*, 13(5), pp.556–560.

Schmitz, I. et al., 2013. IL-21 restricts virus-driven Treg cell expansion in chronic LCMV infection. *PLoS pathogens*, 9(5), p.e1003362.

Schmitz, J.E. et al., 1999. Control of viremia in simian immunodeficiency virus infection by CD8+ lymphocytes. *Science*, 283(5403), pp.857–860.

Seddiki, N. & Lévy, Y., 2018. Therapeutic HIV-1 vaccine: time for immunomodulation and combinatorial strategies. *Current opinion in HIV and AIDS.* Available at: http://dx.doi.org/10.1097/COH.0000000000000444.

Seung, E. et al., 2013. PD-1 Blockade in Chronically HIV-1-Infected Humanized Mice Suppresses Viral Loads. *PloS one*, 8(10), p.e77780.

Sevilla, N. et al., 2004. Viral targeting of hematopoietic progenitors and inhibition of DC maturation as a dual strategy for immune subversion. *The Journal of clinical investigation*, 113(5), pp.737–745.

Sharpe, A.H. et al., 2007. The function of programmed cell death 1 and its ligands in regulating autoimmunity and infection. *Nature immunology, 8(3), pp.239–245.*

Shin, H. et al., 2007. Viral antigen and extensive division maintain virus-specific CD8 T cells during chronic infection. *The Journal of experimental medicine*, 204(4), pp.941–949.

Shin, H. & Wherry, E.J., 2007. CD8 T cell dysfunction during chronic viral infection. *Current opinion in immunology, 19(4), pp.408–415.*

Siewe, B. et al., 2013. Regulatory B cell frequency correlates with markers of HIV disease progression and attenuates anti-HIV CD8+ T cell function in vitro. *Journal of leukocyte biology, 93(5), pp.811–818.*

Smith, H. et al., 1991. Effector and regulatory cells in autoimmune oophoritis elicited by neonatal thymectomy. Journal of immunology , 147(9), pp.2928–2933.

Speiser, D.E. et al., 2014. T cell differentiation in chronic infection and cancer: functional adaptation or exhaustion? *Nature reviews. Immunology, 14(11), pp.768–774.*

Spiropoulou, C.F. et al., 2002. New World arenavirus clade C, but not clade A and B viruses, utilizes alpha-dystroglycan as its major receptor. *Journal of virology, 76(10), pp.5140–5146.*

Sugimoto, M.A. et al., 2016. Resolution of Inflammation: What Controls Its Onset? *Frontiers in immunology*, 7, p.160.

Suri-Payer, E. et al., 1998. CD4+CD25+ T cells inhibit both the induction and effector function of autoreactive T cells and represent a unique lineage of

immunoregulatory cells. *Journal of immunology , 160(3), pp.1212–1218.*

T

Teijaro, J.R. et al., 2013. Persistent LCMV infection is controlled by blockade of type I interferon signaling. *Science*, 340(6129), pp.207–211.

Thimme, R. et al., 2002. Viral and immunological determinants of hepatitis C virus clearance, persistence, and disease. *Proceedings of the National Academy of Sciences of the United States of America*, 99(24), pp.15661–15668.

Tinoco, R. et al., 2009. Cell-intrinsic transforming growth factor-beta signaling mediates virus-specific CD8+ T cell deletion and viral persistence in vivo. *Immunity*, 31(1), pp.145–157.

de la Torre, J.C., 2009. Molecular and cell biology of the prototypic arenavirus LCMV: implications for understanding and combating hemorrhagic fever arenaviruses. *Annals of the New York Academy of Sciences*, 1171 Suppl 1, pp.E57–64.

Traub, E., 1936a. AN EPIDEMIC IN A MOUSE COLONY DUE TO THE VIRUS OF ACUTE LYMPHOCYTIC CHORIOMENINGITIS. *The Journal of experimental medicine*, 63(4), pp.533–546.

Traub, E., 1936b. PERSISTENCE OF LYMPHOCYTIC CHORIOMENINGITIS VIRUS IN IMMUNE ANIMALS AND ITS RELATION TO IMMUNITY. *The Journal of experimental medicine*, 63(6), pp.847–861.

Trautmann, L. et al., 2006. Upregulation of PD-1 expression on HIV-specific CD8 T cells leads to reversible immune dysfunction. *Nature medicine*, 12(10), pp.1198–1202.

U

Udyavar, A.R. et al., 2013. Co-expression network analysis identifies Spleen Tyrosine Kinase (SYK) as a candidate oncogenic driver in a subset of small-cell lung cancer. *BMC systems biology, 7(Suppl 5), p.S1.*

Urbani, S. et al., 2006. PD-1 expression in acute hepatitis C virus (HCV) infection is associated with HCV-specific CD8 exhaustion. *Journal of virology*, 80(22), pp.11398–11403.

Utzschneider, D.T. et al., 2013. T cells maintain an exhausted phenotype after antigen withdrawal and population reexpansion. *Nature immunology*, 14(6), pp.603–610.

V

Velu, V. et al., 2008. Enhancing SIV-specific immunity in vivo by PD-1 blockade. *Nature*, 458(7235), pp.206–210.

Virgin, H.W., Wherry, E.J. & Ahmed, R., 2009. Redefining chronic viral infection. *Cell*,

138(1), pp.30–50.

Vollbrecht, T. et al., 2012. Chronic progressive HIV-1 infection is associated with elevated levels of myeloid-derived suppressor cells. *AIDS* , 26(12), pp.F31–7.

W

Waggoner, S.N. et al., 2011. Natural killer cells act as rheostats modulating antiviral T cells. *Nature*, 481(7381), pp.394–398.

Wherry, E.J. et al., 2007. Molecular signature of CD8+ T cell exhaustion during chronic viral infection. *Immunity*, 27(4), pp.670–684.

Wherry, E.J., 2011. T cell exhaustion. *Nature immunology*, 12(6), pp.492–499.

Wherry, E.J. & John Wherry, E., 2011. T cell exhaustion. *Nature immunology*, 131(6), pp.492–499.

Wilson, E.B. et al., 2013. Blockade of chronic type I interferon signaling to control persistent LCMV infection. *Science*, 340(6129), pp.202–207.

Wilson, E.B. & Brooks, D.G., 2010. Translating insights from persistent LCMV infection into anti-HIV immunity. *Immunologic research*, 48(1-3), pp.3–13.

Wilson, E.B. et al., 2012. Emergence of distinct multiarmed immunoregulatory antigen-presenting cells during persistent viral infection. *Cell host & microbe, 11(5), pp.481–491.*

Wing, K. & Sakaguchi, S., 2008. Regulatory T cells. *In Clinical Immunology. pp. 249–258.*

Wing, K. & Sakaguchi, S., 2010. Regulatory T cells exert checks and balances on self tolerance and autoimmunity. *Nature immunology, 11(1), pp.7–13.*

Wynn, T.A. & Vannella, K.M., 2016. Macrophages in Tissue Repair, Regeneration, and Fibrosis. *Immunity*, 44(3), pp.450–462.

Y

Yamazaki, C. et al., 2013a. Critical roles of a dendritic cell subset expressing a chemokine receptor, XCR1. *Journal of immunology* , 190(12), pp.6071–6082.

Yamazaki, C. et al., 2013b. Critical roles of a dendritic cell subset expressing a chemokine receptor, XCR1. *Journal of immunology* , 190(12), pp.6071–6082.

Yao, S., Zhu, Y. & Chen, L., 2013. Advances in targeting cell surface signalling molecules for immune modulation. *Nature reviews. Drug discovery*, 12(2), pp.130–146.

Yi, J.S., Du, M. & Zajac, A.J., 2009. A vital role for interleukin-21 in the control of a chronic viral infection. *Science*, 324(5934), pp.1572–1576.

Yokosuka, T. et al., 2010. Spatiotemporal basis of CTLA-4 costimulatory molecule-mediated negative regulation of T cell activation. *Immunity, 33(3), pp.326–339.*

Youngblood, B., Wherry, E.J. & Ahmed, R., 2012. Acquired transcriptional programming in functional and exhausted virus-specific CD8 T cells. *Current opinion in HIV and*

AIDS, 7(1), pp.50–57.

Yue, F.Y. et al., 2010. HIV-specific IL-21 producing CD4+ T cells are induced in acute and chronic progressive HIV infection and are associated with relative viral control. *Journal of immunology* , 185(1), pp.498–506.

Z

Zajac, A.J. et al., 1998. Viral immune evasion due to persistence of activated T cells without effector function. *The Journal of experimental medicine*, 188(12), pp.2205–2213.

Zeng, M., Haase, A.T. & Schacker, T.W., 2012. Lymphoid tissue structure and HIV-1 infection: life or death for T cells. *Trends in immunology*, 33(6), pp.306–314.

Zehn, D., Utzschneider, D.T. & Thimme, R., 2016. Immune-surveillance through exhausted effector T-cells. *Current opinion in virology, 16, pp.49–54.*

Zhang, B. & Horvath, S., 2005. A general framework for weighted gene co-expression network analysis. *Statistical applications in genetics and molecular biology*, 4, p.Article17.

Zhen, A. et al., 2017. Targeting type I interferon-mediated activation restores immune function in chronic HIV infection. *The Journal of clinical investigation*, 127(1), pp.260–268.

Zhou, X., Lindsay, H. & Robinson, M.D., 2014. Robustly detecting differential expression in RNA sequencing data using observation weights. *Nucleic acids research*, 42(11), p.e91.

Zinkernagel, R.M., 2002. Lymphocytic choriomeningitis virus and immunology. *Current topics in microbiology and immunology*, 263, pp.1–5.

DECLARATION OF CO-AUTHORSHIP

I declare that this thesis has been composed by myself and that it has not been submitted, in whole or in part, in any previous application for a degree. My contributions and those of the other authors to this work have been as follows:

Dr. Andreas Meyerhans and Dr. Jordi Argilaguet designed the project; Mireia Pedragosa performed the experiments and analysed the data; Dra. Anna Esteve-Codina performed the bioinformatics analysis. Mireia Pedragosa wrote the first draft of the manuscript; Dr. Andreas Meyerhans and Dr. Jordi Argilaguet revised the manuscript.